Copper Cation Interactions with Biologically Essential Types of Ligands: A Computational DFT Study

Matěj Pavelka,[†] Milan Šimánek,[†] Jiří Šponer,[‡] and Jaroslav V. Burda*[,†]

Department of Chemical Physics and Optics, Faculty of Mathematics and Physics, Charles University, Ke Karlovu 3, 121 16 Prague 2, Czech Republic, and Institute of Biophysics, Academy of Sciences of the Czech Republic, Královopolská 135, 612 65 Brno, Czech Republic

Received: November 27, 2005; In Final Form: February 1, 2006

This work presents a systematic theoretical study on Cu(I) and Cu(II) cations in variable hydrogen sulfide−aqua−ammine ligand fields. These ligands model the biologically most common environment for Cu ions. Molecular structures of the complexes were optimized at the density functional theory (DFT) level. Subsequent thorough energy analyses revealed the following trends: (i) The ammine complexes are the most stable, followed by those containing the aqua and hydrogen sulfide ligands, which are characterized by similar stabilization energies. (ii) The most preferred Cu(I) coordination number is 2 in ammine or aqua ligand fields. A qualitatively different binding picture was obtained for complexes with H_2S ligands where the 4-coordination is favored. (iii) The 4- and 5-coordinated structures belong to the most stable complexes for Cu(II), regardless of the ligand types. Vertical and adiabatic ionization potentials of Cu(I) complexes were calculated. Charge distribution (using the natural population analysis (NPA) method) and molecular orbital analyses were performed to elucidate the nature of bonding in the examined systems. The results provide in-depth insight into the Cu-binding properties and can be, among others, used for the calibration of bioinorganic force fields.

1. Introduction

The improved quantum-chemical approaches and high performance computers led in the past decades to intensified study of transition-metal complexes in many theoretical laboratories. Copper, despite its toxicity in pure form, is fundamental for the activity of many enzymes, which are important in oxygen transport and insertion, electron transfer, oxidation−reduction processes, and so forth. In some cases, the activity is connected with a relatively high electron affinity and the Cu(II) oxidation state can be easily reduced to Cu(I). There are many theoretical and experimental studies exploring copper proteins. For instance, Siegbahn et al.[1] studied the redox process on tyrosinase. In another work, the authors studied the molecular mechanism of the oxidation reaction on a center of copper amine oxidase using the B3LYP technique.[2] Wang et al. studied the importance of histidine ligands in a Cu center of azurin using ultraviolet−visible (UV−vis) and electron paramagnetic resonance (EPR) spectra.[3] In Solomon's group,[4] spectroscopic tools in combination with density functional theory (DFT) calculations were used to investigate the role of an amino acid in the axial position to the copper complex and its influence on the reduction potential. Similarly, the plastocyanin model complexes were examined in studies,[5,6] where also several spectroscopic techniques in combination with DFT calculations were applied. The calculations have confirmed the role of ligand−metal charge transfer (LMCT) S $p\pi \rightarrow$ Cu on various spectra intensities. The related experimental works from Tolman's group should also be mentioned.[7,8] The basic aspects of a copper coordination in blue proteins are summarized in a short review.[9] A lot of computational effort was devoted to studies of blue proteins by Olsson et al.[10−13] An interesting study of plastocyanin and rusticyanin was performed by Olsson and Warshel,[10] where an approach to computing the reduction potential is presented. A pump−probe study of CT dynamics in the excited state was carried out by Book et al.[14] The wave-resolved signal of vibration on 500 cm^{-1} was assigned to the excited-state lifetime in a copper complex of plastocyanin and ceruloplasmin in spinach. Also, Fraga et al.[15] studied the CT dynamics of plastocyanin using resonance Raman spectroscopy.

Some other theoretical studies of the copper interactions with amino acids have been reported recently, including an attempt to explain the nonplanar arrangement of the copper(II) complexes with amino acids in crystal structures using the ab initio method and molecular mechanics.[16] The same authors have published a new force field parametrization of Cu(II)[17] based on gas phase B3LYP calculations. Plenty of inspiration can be found in a study of Glusker's group on copper-binding motifs.[18] A similar combination of database structures and quantum-chemical calculations can be found in very extensive studies performed by Rulíšek et al.[19−22] The Cu(I)−Cu(II) bonding in relation to glycine was scrutinized by Bertran et al.[23] Shoeib et al.[24] studied the Cu^+/Ag^+ cation interactions with glycine molecules using the B3LYP/PVDZ method. They showed that while the Ag^+ cation prefers 3- and 4-coordinated complexes, a lower coordination (2) occurs in the Cu^+ cases. The same group also examined some other aspects of Cu interactions.[25]

Many experimental works were published on the coordination of copper cations with various amino acids. Among others, a recent study of Santra et al.[26] should be mentioned. The authors dealt with the interactions of the Cu^{2+}(glutamate) complex with cyclodextrine and benzonitrile using the fluorescence spectroscopy. EPR and electron−nuclear double resonance (ENDOR) techniques were used[27] to determine Cu(II)−histidine complexes. Six-membered chelating rings are formed when histidine

* Corresponding author. E-mail: burda@karlov.mff.cuni.cz.
[†] Charles University.
[‡] Academy of Sciences of the Czech Republic.

10.1021/jp056868z CCC: $33.50
Published on Web 03/22/2006

molecules bind the Cu^{2+} cation. X-ray absorption near-edge structure (XANES) spectra for a series of Cu(II) compounds[28] were utilized to interpret a ligand field theory in the explored Cu(II) compounds. Sigman et al.[29] have examined the Cu(II) coordination site in cytochrome *c* peroxidase with EPR and UV−vis spectra.

A great deal of work is devoted to the examination of copper complexes with DNA/RNA bases. IR spectra were measured and interpreted for interactions of DNA with several divalent cations in a solution.[30] The crystal structures of several metal complexes and DNA cleaving activity were characterized in study.[31] Thermodynamical measurements[32] on nucleosides coordinated with Ca and Cu divalent cations suggest the following order in bonding strength: $Cu^{2+} > Ca^{2+}$ and GMP > IMP > AMP > CMP = UMP for the nucleotides. Formation of macrochelates was found to be energetically favorable but entropically unfavorable. Melting curves of copper(II) linked in a duplex DNA oligomer were measured in a study of Meggers et al.[33] The same authors have also explored the structural aspects of a copper(II) coordination influence on Watson−Crick (WC) base pairing.[34] The interactions of the polynuclear copper-(I) complexes with double-stranded DNA oligomers were explored by Lehn's group.[35]

A theoretical study of Cu^{2+} association with uracil and its thio derivatives has been published recently.[36] Coordination and stability of Cu(II) and Zn(II) complexes with adenosine and cytidine were investigated by Gasowska.[37] Binding of Cu^{+} cations to guanine and adenine,[38] WC AT and GC base pairs,[39] and in a noncomplementary DNA C−A base pair[40] was explored in our previous studies. Recently, Noguera[41] examined WC GC base pair interacting with Ca^{2+}, Cu^{+}, and Cu^{2+} cations where both naked and hydrated cations were considered. The outer-shell and inner-shell coordination of a phosphate group to hydrated metal ions (Mg^{2+}, Cu^{2+}, Zn^{2+}, Cd^{2+}) in the presence and absence of nucleobase was explored in the work of Rulíšek.[42] Hydrated Cu(I) association to guanine has been published recently.[43]

Small inorganic complexes of Cu cations are also intensively studied. Many works (already mentioned in our previous studies) are devoted to the study of the coordination geometries and/or electronic properties of Cu cations interacting with molecules such as water or ammonia[44−64] using various computational approaches. In our previous papers,[65,66] hydration of both Cu(I) and Cu(II) cations and their interactions with variable ammonia−water surroundings were systematically examined.

The present study provides a new detailed investigation of Cu(I)/Cu(II) interactions with an extended sulfide−aqua−ammine ligand field. Structural, thermodynamic, and electronic properties are determined and used to characterize such copper complexes. A comparison with previous results underlines new qualitative features which appear in the presence of coordinated sulfur-containing ligands. This work thus provides an important approximate model for copper interactions with amino acids such as histidine, methionine, cysteine, and glutamine or other bioenvironments.

2. Computational Details

The $[Cu(H_2S)_m(H_2O)_n(NH_3)_k]^{2+}$ complexes were studied, where *n*, *m*, and *k* were equal to 0, 2, 4, or 6 with the $m + n + k$ sum being 4 or 6. In the case of Cu(I) complexes, these systems were reduced to four molecules in a metal proximity, since stable Cu(I) compounds with higher coordination numbers are very rare. Some additional calculations were carried out with uneven numbers of ligands. Note also that in some calculations a ligand was drifted to the second hydration shell, which leads to an uneven number of ligands in the first ligand shell.

In many cases, we attempted multiple gradient optimizations utilizing different starting geometries. This often resulted in distinct local minima. However, only the lowest energy conformer for every coordination number was considered in the further analyses.

Quantum-chemical calculations were performed at the density functional theory (DFT) level using the B3PW91 functional. For the H, O, and N atoms, the 6-31+G(d) basis set was applied. The copper and sulfur core electrons were described by Christiansen averaged relativistic effective pseudopotentials (AREP).[67] A consistent basis set was adopted for the valence electrons. Double-ζ pseudoorbitals of Cu were augmented by diffuse and polarization functions ($\alpha_s = 0.025$, $\alpha_p = 0.35$, $\alpha_d = 0.07$, and $\alpha_f = 3.75$).[68] Similarly, pseudoorbitals of the sulfur atom were extended by analogous functions with exponents: $\alpha_s = 0.077$, $\alpha_p = 0.015$, and $\alpha_d = 0.50$.

Compounds with the Cu^{+} cation are represented by a closed-shell singlet electronic ground state. Cu(II) complexes contain copper in the $3d^9$ electron configuration resulting in doublet ground states. A lot of attention was devoted to the construction of an appropriate initial guess for the self-consistent field (SCF) procedure. First, the correct wave function was constructed in a minimal basis set using the restricted open-shell Hartree−Fock (ROHF) method, going subsequently to the final unrestricted B3PW91/6-31+G(d) level.

Energy and charge distribution analyses were calculated with the B3LYP functional and extended 6-311++G(2df,2pd) basis set for the H, N, and O atoms. Consistently, the basis sets on the copper/sulfur atoms were enlarged by spd/sp diffuse functions and 2fg,2df polarization functions ($\alpha_f = 4.97, 1.30$, $\alpha_g = 3.28/\alpha_d = 0.92, 0.29$, $\alpha_f = 0.57$).[65] Recently, new studies have appeared where BHLYP is recommended over B3LYP;[69] however, no substantial difference was found in our case for selected test systems.

The energetics of interactions was evaluated on the basis of several quantities. First, the conventional stabilization energies with the basis set superposition error (BSSE) corrections and corrections on the deformation energies[70] were determined according to the equation

$$\Delta E^{\mathrm{stab}} = -(E_{\mathrm{complex}} - \sum E_{\mathrm{monomer}} - \sum E^{\mathrm{deform}}) \qquad (1)$$

where E_{complex} represents total energy of the whole complex and E_{monomer} represents the energy of a given subsystem computed with basis functions on the ghost atoms from the complementary part of the system. Besides the ΔE^{stab} energies, we also computed coordination energies ($\Delta E^{\mathrm{coord}}$) and *st*abilization energies with *ex*clusion of sterical repulsion and weak associative interactions (ΔE^{stex}). The coordination energies were evaluated for the Cu(I) systems, where ligand molecules often escape to the second solvation shell. In such calculations, only directly bonded (first-shell) ligands were considered in eq 1 using the optimized geometry of the whole complex. The ΔE^{stab} and $\Delta E^{\mathrm{coord}}$ terms are identical when all ligands remain in the first shell. ΔE^{stex} is obtained when all of the interacting ligand molecules are treated in eq 1 as one subsystem and the central Cu ion as another one. That is, this energy is equal to the binding energy of the cation with a given ligand shell. The ΔE^{stex} energy was evaluated only for the Cu(II) complexes where a higher coordination causes an increased electrostatic repulsion of the ligands. The difference between ΔE^{stab} and ΔE^{stex} then basically reflects the energy investment that would be necessary to form the ligand-shell arrangement in the absence of the ion.

Note, however, that the actual interligand repulsion in the presence of the Cu cation is even larger, due to interligand electrostatic repulsion caused by the polarization/charge transfer effects of the metal cation. For further discussion on the estimation of polarization and CT energies, the studies of Tiraboschi[71,72] or Šponer[73] can be used. In addition, the bonding energies (ΔE^{BE}) were estimated using the same (BSSE) scheme of eq 1 but without the monomer deformation corrections. In this energy determination, partition of the complex to two parts (ligand and the rest of the complex) splits the examined Cu−X bond, giving the binding energy of the desired ligand. Only 4-coordinated Cu(I) and Cu(II) complexes were considered for comparison. Various energy evaluation schemes, as specified above, allow a more thorough insight into the balance of forces in the calculated systems.

Further vertical and adiabatic ionization potentials (IPs) were calculated for the monovalent copper compounds according to formula 2:

$$\mathrm{IP} = E_{\mathrm{Cu(II)}} - E_{\mathrm{Cu(I)}} \qquad (2)$$

In the case of the vertical IP, the $E_{\mathrm{Cu(II)}}$ term represents the energy of a (2+) charged system calculated in the Cu(I) optimized structure. For the adiabatic IP, the $E_{\mathrm{Cu(II)}}$ energy was computed using the Cu(II) optimized structure. For the sake of consistency, selected electron affinities were also calculated. Determined IPs and electron affinities (EAs) were compared with energies based on Koopmans' theorem and values calculated based on outer valence Green function propagators in the 6-31+G(d) basis set. The method is based on the eigenvalue of the canonical molecular orbital (MO) (highest occupied molecular orbital (HOMO) for IP or lowest unoccupied molecular orbital (LUMO) for EA) from Koopmans' theorem corrected by algebraic expressions similar to perturbation theory.[74,75]

For deeper insight into the electronic properties of the examined systems, molecular orbitals and electrostatic potentials were analyzed. Further, partial charges and spin densities on atoms were determined using the natural population analysis (NPA) method.[76] The program package Gaussian 98[77] was used for all quantum-chemical calculations, and the program NBO v. 5.0 from Wisconsin University[78] was used for evaluation of the natural bond orbital (NBO) characteristics. Visualization of geometries, MOs, vibrational modes, and maps of electrostatic potentials was performed using the Molden 4.4[79] and Molekel 4.3[80,81] programs.

3. Results and Discussion

3.1. Structural Parameters. All geometries reported in this paper are available in the Supporting Information. The present calculations thus can be easily used for the verification/calibration of lower quality methods, and they can be easily extended, for example, for a subset of structures, by higher level calculations.

First, structures of the Cu(I) and Cu(II) complexes coordinated exclusively with H_2S molecules were studied. These systems contain copper with $(H_2S)_n$ molecules considering the coordination number (n) varying from 1 to 4 in the Cu(I) complexes and from 1 to 6 in the Cu(II) complexes. The structures of these compounds are displayed in Figure 1 for Cu(I) and in Figure 2 for Cu(II). For the $[Cu(H_2S)]^+$ complex (**1a**), the coordination distance (2.21 Å) can be compared with the results of Hamilton's[45] study, where a shorter Cu−S bond (2.13 Å) is reported using the DFT(B3P86/DZP) method. For the $[Cu(H_2S)]^{2+}$ (**2a**) and $[Cu(H_2S)_2]^{2+}$ (**2b**) structures, Cu−S distances of 2.32 and 2.29 Å were obtained. The explanation of the shorter Cu−S bonds in a 2-coordinated Cu(II) system compared to a single-ligated complex is in section 3.5 below and was also discussed in previous studies.[65,66] For higher coordination numbers, the bond lengths elongate monotonically with the increasing number of ligands from 2.2 to 2.4 Å in the Cu(I) complexes and from 2.3 to 2.5 Å in the Cu(II) complexes. All optimized Cu−S distances are presented in Table 1.

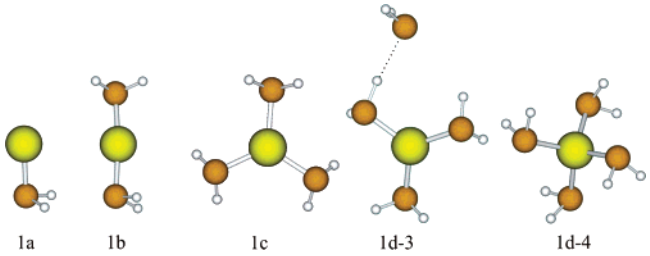

Figure 1. Homoligated Cu(I) complexes with hydrogen sulfide ligands.

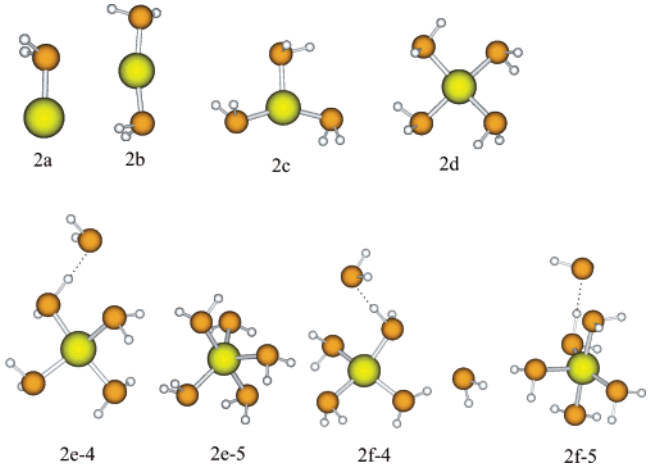

Figure 2. Homoligated Cu(II) complexes with hydrogen sulfide ligands.

It is interesting to mention that monovalent copper forms shorter Cu−S bonds than its divalent cation. On the other hand, in copper−water−ammonium complexes, the bonds of Cu^+ cation are longer (cf. refs 65 and 66). An explanation of the shorter Cu−S distances in monovalent complexes can be seen in the fact that the sulfur atom (still) keeps a negative partial charge in the Cu^+ complexes. On the contrary, in the $[Cu(H_2S)]^{2+}$ complex, a positive partial charge is located on the sulfur atom. This means that partial electrostatic repulsion is responsible for the elongation of the Cu−S bond in this complex. With the increasing number of ligands in the $[Cu(H_2S)_n]^{2+}$ complexes, the partial charge on sulfur atoms decreases up to $-0.2e$. Nevertheless, a less negative partial charge can always be found in the Cu(II) complexes as compared with the corresponding Cu(I) ones. Moreover, for donor−acceptor bonding, the polarizability or softness/hardness characterization must also be considered. The hardness of H_2S is about 6.2. It matches the Cu^+ value of 6.3. On the other hand, the Cu^{2+} cation keeps the electrons more tightly and the hardness increases to 8.3 (the data are taken from the work of Pearson[82]). Therefore, the higher covalent contribution of the Cu−S bond results in shorter bond lengths in the Cu(I) complexes. Water and ammonia are more polar molecules ($\mu = 1.92$ and 1.53, respectively) in comparison with the H_2S molecule ($\mu = 1.08$ D at the B3LYP/6-311++G-(2df,2pd) level of theory). Therefore, a strong electrostatic contribution to the Cu−O/Cu−N bonds leads to a shorter distance in the case of Cu^{2+}.

TABLE 1: Selected Parameters of $[Cu(H_2S)_n]^{2+/+}$ Complexes: Cu−S Distances (in Å), ΔE^{stab}, ΔE^{stex}, and ΔE^{coord} Energies (in kcal/mol, See Method for Definition), Occupation of 4s (and 3d) Copper AO, Partial Charges δ(Cu), and Spin Densities ρ_S(Cu) (in *e*)[a]

system	c.n.	struct	Cu−S	ΔE^{stab}	ΔE^{coord}	4s	δ(Cu)
$[Cu(H_2S)]^+$	1	**1a**	2.208	49.1	49.1	0.27	0.79
$[Cu(H_2S)_2]^+$	2	**1b**	2.221, 2.221	90.5	90.6	0.53	0.57
$[Cu(H_2S)_3]^+$	3	**1c**	2.300, 2.301, 2.304	103.3	103.2	0.44	0.62
$[Cu(H_2S)_4]^+$	3	**1d-3**	2.291, 2.302, 2.305	108.6	102.9	0.45	0.61
	4	**1d-4**	2.386, 2.388, 2.388, 2.388	110.3	110.4	0.43	0.60

system	c.n.	struct	Cu−S	ΔE^{stab}	ΔE^{stex}	4s	3d	δ(Cu)	ρ_S(Cu)
$[Cu(H_2S)]^{2+}$	1	**2a**	2.323	146.4	146.4	0.12	9.58	1.29	0.44
$[Cu(H_2S)_2]^{2+}$	2	**2b**	2.291, 2.291	223.5	224.2	0.39	9.39	1.19	0.73
$[Cu(H_2S)_3]^{2+}$	3	**2c**	2.360, 2.314, 2.309	276.0	280.5	0.53	9.53	0.91	0.44
$[Cu(H_2S)_4]^{2+}$	4	**2d**	2.391, 2.403, 2.406, 2.425	303.6	313.9	0.53	9.56	0.87	0.40
$[Cu(H_2S)_5]^{2+}$	4	**2e-4**	2.333, 2.397, 2.415, 2.439	317.2	331.5	0.53	9.56	0.87	0.40
	5	**2e-5**	2.425, 2.442, 2.488, 2.492, 2.548	318.3	333.3	0.53	9.55	0.86	0.41
$[Cu(H_2S)_6]^{2+}$	4	**2f-4**	2.337, 2.382, 2.406, 2.414	329.4	346.3	0.52	9.58	0.86	0.38
	5	**2f-5**	2.411, 2.434, 2.446, 2.488, 2.592	329.4	347.2	0.53	9.56	0.86	0.40

[a] The abbreviation c.n. is used for coordination number, and struct corresponds to the identification number used in Figures 1−5.

The 2-coordinated structures deviate from the assumed linearity by approximately 10°. The 3-coordinated Cu(I) complex (**1c**) has practically C_s symmetry in the heavy-atom backbone with the same Cu−S distance (2.30 Å). The Cu(II) structure (**2c**) resembles a deformed planar T shape with one of the Cu−S distances elongated to 2.36 Å. The global minimum for the 4-coordinated Cu(I) complex (**1d-4**) was obtained in a near tetrahedral conformation with equal Cu−S bond lengths. In the $[Cu(H_2S)_4]^+$ system, other (less) stable structures with a coordination number of 3 were found. The geometry of the most stable one is illustrated in Figure 1 (**1d-3**). The H···S distance between the first- and second-shell ligands is relatively long in the Cu(I) (**1d-3**) structure, about 2.44 Å. The global minimum of the $[Cu(H_2S)_4]^{2+}$ cation (**2d**) has distorted square-planar configurations with a dihedral angle of ∼20°. Interestingly, no stable 6-coordinated Cu(II) complex was found. The 5-coordinated structures favor a distorted tetragonal-pyramid arrangement with one of the equatorial Cu−S bonds elongated (**2e-5** and **2f-5**). Unlike in hexaaqua−copper complexes, the outer H_2S molecule does not prefer the formation of H-bonded cross-links and remains coordinated to only one first-shell ligand. For the Cu(II) complexes, H-bond lengths vary from 1.98 to 2.10 Å.

The angle between the H_2S plane and Cu−S bond increases with the increasing number of ligand molecules (from 104 to 111°) in the Cu(I) structures. In the $[Cu(H_2S)n]^{2+}$ systems (n = 2−6), the angles are generally slightly larger and vary from 106 to 112°. However, the largest angle (118°) was found in the monosulfide Cu(II) compound (**2a**). A different situation occurred in our previous study,[65] where purely aqua ligands were explored. Angles of 172 and 154° were observed in the $[Cu(H_2O)]^+$ and $[Cu(H_2O)]^{2+}$ complexes, while angles of 104 and 118° occur in $[Cu(H_2S)]^+$ and $[Cu(H_2S)]^{2+}$, respectively. In the remaining Cu(II) aqua complexes, the angles were larger—up to about 176°. Such an angle is the result of two competing factors: (a) the angle corresponding to a dative bond tends to be ∼109° (according to the tetrahedral sp^3 hybridization of water or hydrogen sulfide), and (b) the electrostatic term, based on a metal−ligand/monopole−dipole moment interaction, favors an angle of 180°. Larger angles of aqua ligands can be explained by a prevailing role of electrostatic factors, while in the H_2S complexes the dative character clearly dominates. The similar structures were described in the case of Zn^{2+} by Pullman et al.[83] or later by Gresh[84,85]

In the next part, systems with a variable sulfide−aqua−ammine ligand field were explored. For the $[Cu(H_2S)_m(H_2O)_n(NH_3)_k]^+$ systems, stable 2-, 3-, and 4-coordinated geometries were localized. However, in the $[Cu(H_2S)_4]^+$ system (**1d** = **3a**), no stable 2-coordinated structure exists. On the contrary, for the $[Cu(H_2O)_2(NH_3)_2]^+$ complex (**3g**), no 4-coordinated structure was found. The obtained Cu−X (X = S, O, and N) bond lengths of the most stable structures are compiled in the upper part of Table 2, and the optimized structures are depicted in Figure 3.

Generally, bond lengths increase with increasing coordination number. For the 2-, 3-, and 4-coordinated structures, the Cu−S distances vary from 2.2 to 2.4 Å, respectively. The same behavior was found for Cu−NH_3, where bonds elongate from 1.9 to 2.1 Å. The Cu−O distances display the largest variability changing from 1.9 to 2.4 Å. On the basis of the optimized structures, it can be concluded that the most preferred ligand (most frequently occurring in the first solvation shell) is ammonia followed by H_2S (for both Cu(I) and Cu(II) cations), leaving water as the least favored ligand.

Optimized structures of the divalent $[Cu(H_2S)_m(H_2O)_n(NH_3)_k]^{2+}$ complexes (where $m + n + k = 4$ or 6) are presented in the lower part of Table 2 and in Figures 4 and 5. The 4-coordinated Cu(II) complexes favor partially deformed square-planar geometry in contrast to the tetrahedral structures of Cu(I). Such a conclusion can also be found in some other works, for example, in ref 86.

To determine the ligand arrangement of the 5-coordinated structures, the Cu−X metal−ligand distances and X−Cu−X angles have been measured. Trigonal bipyramid reveals an angle distribution close to 180 and 120°. This arrangement was found only in the $[Cu(H_2S)_4(NH_3)_2]^{2+}$ (**5h-5**) complex. In all other cases, a distorted octahedral configuration was found with an angle distribution close to 90 and 180°. More quantitative expression can be based on evaluation of the so-called τ-parameter, which is defined as $\tau = (\theta - \varphi)/60°$. Here, the θ and φ angles are the two largest valence angles in the complex. From Table 3, it can be seen that the only τ value larger than 0.6 is for the **5h-5** structure. Two borderline structures with τ values around 0.4−0.6 are the $[Cu(H_2S)_6]^{2+}$ and $[Cu(H_2S)_2(H_2O)_2(NH_3)_2]^{2+}$ complexes which "optically" can be considered closer to the tetragonal-pyramid shape.

The structures with six directly bonded molecules (**5b-6**, **5c-6**, **5d-6**, **5e-6**, and **5f-6**) exhibit distorted O_h symmetry with the axial bonds elongated due to the Jahn−Teller effect known from classical textbooks. However, in three cases—$[Cu(H_2S)_6]^{2+}$,

TABLE 2: Copper−Ligand Distances (in Å) for the Cu(I) and Cu(II) Complexes[a]

system	c.n.	struct	Cu−lig1	Cu−lig2	Cu−lig3	Cu−lig4	Cu−lig5	Cu−lig6
$[Cu(H_2S)_4]^+$	3	**3a-3**	2.291*	2.302*	2.305*			
	4	**3a-4**	2.386*	2.388*	2.388*	2.388*		
$[Cu(H_2S)_2(H_2O)_2]^+$	2	**3b-2**	2.200*	2.219*				
	3	***3b-3***	*2.247**	*2.284**	*2.050***			
	4	**3b-4**	2.282*	2.286*	2.172**	2.282**		
$[Cu(H_2S)_2(H_2O)(NH_3)]^+$	2	**3c-2**	1.922	2.193*				
	3	***3c-3***	*2.022*	*2.271**	*2.327**			
	4	**3c-4**	2.043	2.310*	2.312*	2.435**		
$[Cu(H_2S)_2(NH_3)_2]^+$	*2*	***3d-2***	*1.912*	*1.912*				
	3	**3d-3**	2.041	2.044	2.287*			
	4	**3d-4**	2.105	2.119	2.383*	2.385*		
$[Cu(H_2O)_4]^+$	*2*	***3e-2***	*1.878***	*1.878***				
	3	**3e-3**	1.970**	1.976**	2.143**			
	4	**3e-4**	1.998**	2.085**	2.207**	2.257**		
$[Cu(H_2O)_2(NH_3)_2]^+$	*2*	***3f-2***	*1.909*	*1.909*				
	3	**3f-3**	1.944	1.944	2.349**			
$[Cu(NH_3)_4]^+$	*2*	***3g-2***	*1.905*	*1.905*				
	3	**3g-3**	1.998	2.073	2.078			
	4	**3g-4**	2.136	2.136	2.136	2.136		
$[Cu(H_2S)_4]^{2+}$	4	**4a**	2.391*	2.403*	2.406*	2.425*		
$[Cu(H_2S)_2(H_2O)_2]^{2+}$	4	**4b**	2.354*	2.360*	1.996**	2.052**		
$[Cu(H_2S)_2(H_2O)(NH_3)]^{2+}$	4	**4c**	2.008	2.429*	2.351*	2.090**		
$[Cu(H_2S)_2(NH_3)_2]^{2+}$	4	**4d**	2.007	2.019	2.455*	2.467*		
$[Cu(H_2O)_4]^{2+}$	4	**4e**	1.957**	1.959**	1.960**	1.963**		
$[Cu(H_2O)_2(NH_3)_2]^{2+}$	4	**4f**	2.003	2.003	2.023**	2.023**		
$[Cu(NH_3)_4]^{2+}$	4	**4 g**	2.051	2.051	2.051	2.051		
$[Cu(H_2S)_6]^{2+}$	4	**5a-4**	2.382*	2.337*	2.406*	2.414*		
	5	***5a-5***	*2.411**	*2.434**	*2.446**	*2.488**	*2.592**	
$[Cu(H_2O)_6]^{2+}$	*4*	***5b-4***	*2.033***	*2.033***	*2.033***	*2.033***		
	5	**5b-5**	1.957**	1.963**	2.074**	2.081**	2.086**	
	6	**5b-6**	1.984**	1.984**	2.010**	2.010**	2.242**	2.242**
$[Cu(NH_3)_6]^{2+}$	*4*	***5c-4***	*2.042*	*2.043*	*2.043*	*2.044*		
	5	**5c-5**	2.071	2.071	2.098	2.099	2.285	
	6	**5c-6**	2.171	2.171	2.174	2.174	2.512	2.512
$[Cu(H_2S)_2(H_2O)_4]^{2+}$	*4*	***5d-4***	*2.356**	*2.389**	*1.955***	*1.997***		
	5	**5d-5**	2.380*	2.411*	2.024**	2.037**	2.219**	
	6	**5d-6**	2.408*	2.408*	2.054**	2.054**	2.353**	2.353**
$[Cu(H_2S)_4(H_2O)_2]^{2+}$	*4*	***5e-4***	*2.398**	*2.390**	*2.410**	*2.379**		
	5	**5e-5**	2.434*	2.435*	2.439*	2.440*	2.191**	
	6	**5e-6**	2.426*	2.437*	2.438*	2.477*	2.376**	2.477**
$[Cu(H_2S)_2(H_2O)_2(NH_3)_2]^{2+}$	*4*	***5f-4***	*2.011*	*2.018*	*2.431**	*1.981***		
	5	**5f-5**	2.009	2.014	2.527*	2.611*	2.118**	
	6	**5f-6**	2.011	2.011	2.532*	2.533*	2.429**	2.596**
$[Cu(H_2S)_2(NH_3)_4]^{2+}$	*4*	***5g-4***	*2.046*	*2.047*	*2.053*	*2.053*		
	5	**5g-5**	2.059	2.062	2.077	2.080	2.840*	
$[Cu(H_2S)_4(NH_3)_2]^{2+}$	*4*	***5h-4***	*2.014*	*2.015*	*2.430**	*2.440**		
	5	**5h-5**	2.018	2.025	2.489*	2.608*	2.608*	

[a] The abbreviation c.n. represents the coordination number, and struct specifies the optimized structure. Italic font indicates the global minimum. One asterisk denotes Cu−S bond lengths, and two asterisks denote Cu−O bond lengths, while all remaining values are those for Cu−N bonds.

$[Cu(H_2S)_4(NH_3)_2]^{2+}$, and $[Cu(H_2S)_2(NH_3)_4]^{2+}$—no stable 6-coordinated geometries have been found.

The Cu(II)−ligand distances are presented in the second part of Table 2. Generally, Cu−S bond lengths in mixed 4-coordinated complexes are approximately 2.4 Å long. Cu−N distances are about 2.0−2.1 Å, and Cu−O bonds are in the range 2.0−2.4 Å. They again display the largest variability. If the number of ligated molecules is higher than four, the analogous trends remain valid. However, individual distances exhibits higher variability; the bonds elongate typically to 2.84, 2.51, and 2.35 Å for the Cu−S, Cu−N, and Cu−O bonds, respectively.

Katz's work[18] presents the optimized 4-coordinated $[Cu(H_2S)_m(NH_3)_n]^{2+/+}$ complexes (where $m + n = 4$) at the MP2/LANL2DZ+d level, which can be confronted with our structures. They have found values of 2.36 and 2.45 Å for the Cu−S bonds in the $[Cu(H_2S)_4]^{2+}$ and $[Cu(H_2S)_2(NH_3)_2]^{2+}$ systems, respectively. The values are in good agreement with the present distances (2.41 and 2.46 Å). However, they report the tetrahedral geometries in comparison with the distorted square-planar structures found in our study. In the case of Cu(I) compounds, the Cu−S bonds differ only slightly: 2.42 and 2.44 Å versus 2.39 and 2.38 Å (this work) for $[Cu(H_2S)_4]^+$ and $[Cu(H_2S)_2(NH_3)_2]^+$, respectively.

The extensive study of Katz et al.[18] also examines approximately 6000 entries in the Cambridge Structural Database (CSD). More than 50% of the mentioned Cu(I) structures are of the 4-coordinated type. The rest is divided between 2- and 3-coordinated complexes. The ligands with coordinated nitrogen (60%) and sulfur (35%) elements are preferred. For the Cu(II) entries, the most usual are 4- and 5-ligated complexes and only about 25% belongs to octahedral (6-coordinated) structures. In these octahedral complexes, copper is preferably coordinated with a ligand by the oxygen (50%) and nitrogen (50%) atoms. The database also indicates the copper−ligand bond lengths. Table 4 compares our averaged Cu−X (S, O, N) distances with the corresponding CSD values for both Cu^+ and Cu^{2+} cations with various coordination numbers. The

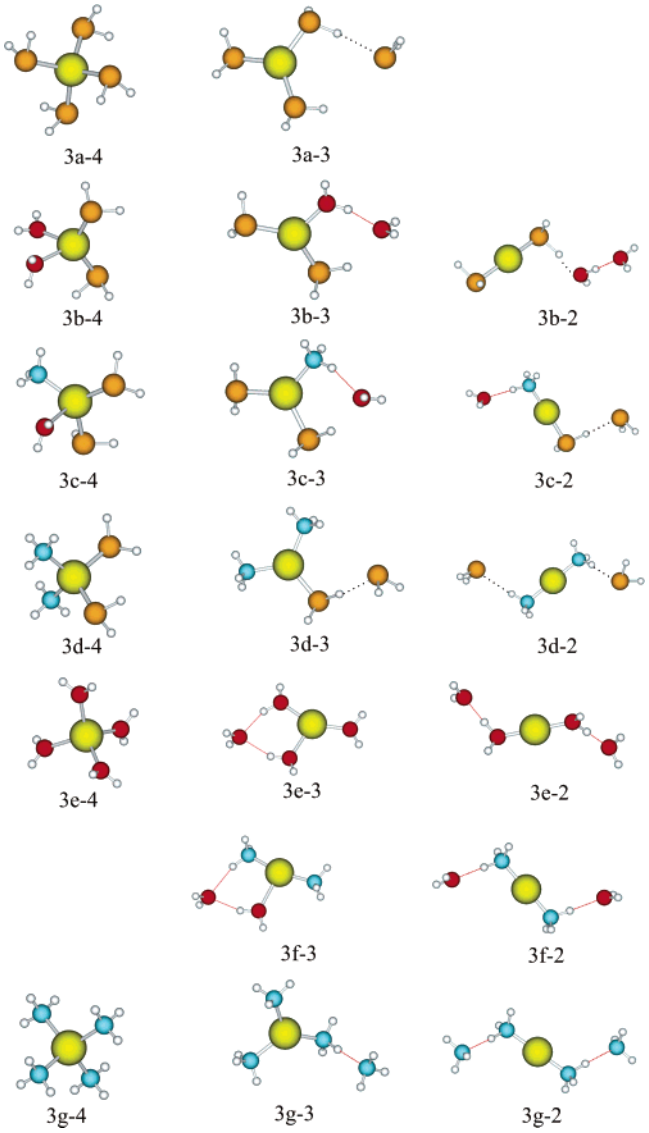

Figure 3. Cu(I) complexes containing mixed ligand molecules.

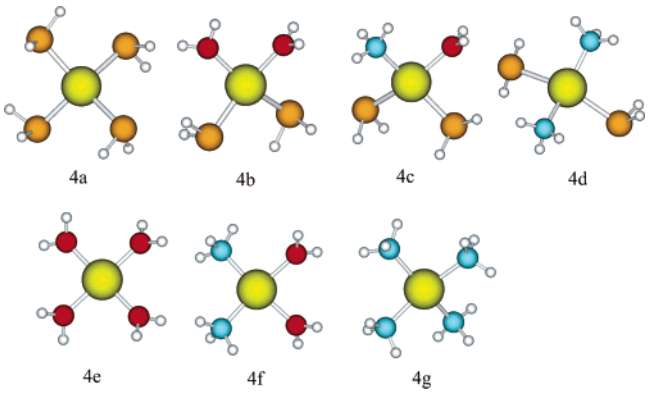

Figure 4. Cu(II) complexes with four mixed ligand molecules.

calculated bond lengths match well with the data presented in the database.

3.2. Stabilization Energies. Energy parameters of purely hydrogen sulfide systems $[Cu(H_2S)_n]^{2+/+}$ are listed in Table 1. Figure 6 shows the dependence of the ΔE^{stab} stabilization energies on the number of coordinated ligands for the Cu(I) complexes. An analogous plot in the case of the Cu(II) compounds is displayed in Figure 7. In the case of both monovalent and

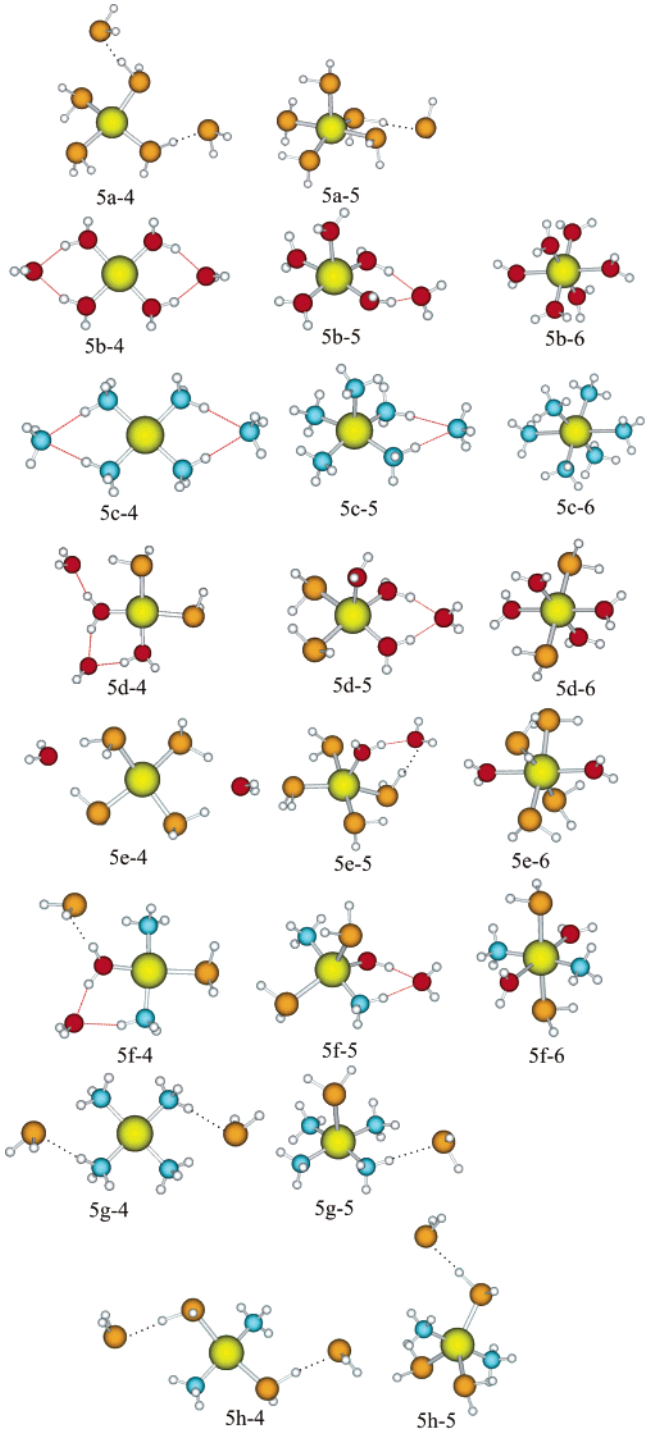

Figure 5. Cu(II) complexes with six mixed ligand molecules.

divalent complexes, stabilization energy increases with an increasing number of directly bonded molecules.

Hamilton[45] found the stabilization of the $[Cu(H_2S)]^+$ complex to be about 50 kcal/mol using B3P86 and the polarized double-ξ basis set. The value is in very good agreement with the presented result (49 kcal/mol) despite the fact that the Cu−S bond length was found to be different by almost 0.1 Å (see above).

When compared to previous calculations, where only water and ammonia molecules were included, an important difference can be noticed. The $[Cu(H_2S)_4]^+$ systems prefer the 4-coordinated structures (**1d-4**). The reason is the larger polarizability of the sulfur atom in the H_2S molecule and the higher donation affinity. Simultaneously, the very weak H-bonding cannot compete with the Cu−S dative interactions. Since mutual

TABLE 3: τ-Parameter for the 5-Coordinated Cu(II) Complexes[a]

system	struct	θ	φ	τ
$[Cu(H_2S)_6]^{2+}$	**5a-5**	177.3	152.2	0.42
$[Cu(H_2O)_6]^{2+}$	**5b-5**	170.9	165.5	0.09
$[Cu(NH_3)_6]^{2+}$	**5c-5**	163.0	163.0	0.00
$[Cu(H_2S)_2(H_2O)_4]^{2+}$	**5d-5**	172.5	160.9	0.19
$[Cu(H_2S)_4(H_2O)_2]^{2+}$	**5e-5**	178.8	158.7	0.33
$[Cu(H_2S)_2(H_2O)_2(NH_3)_2]^{2+}$	**5f-5**	174.6	143.6	0.52
$[Cu(H_2S)_2(NH_3)_4]^{2+}$	**5g-5**	172.5	166.7	0.10
$[Cu(H_2S)_4(NH_3)_2]^{2+}$	**5h-5**	179.4	129.8	0.83

[a] θ is the largest valence ligand−metal−ligand angle, and φ is the second largest angle. The abbreviation struct is used for identification of the optimized structures.

TABLE 4: Average Cu−X (S, O, N) Bond Lengths (in Å) and Corresponding Values Obtained from the CSD Database by Katz et al.[18a]

	present			CSD		
Cu(I)	2-coord	3-coord	4-coord	2-coord	3-coord	4-coord
Cu−N	1.91	2.02	2.12	1.90	1.98	2.04
Cu−O	1.88	2.04	2.21	1.84	2.14	2.05
Cu−S	2.19	2.29	2.35	2.17	2.26	2.33

	present			CSD		
Cu(II)	4-coord.	5-coord.	6-coord.	4-coord.	5-coord.	6-coord.
Cu−N	2.03	2.09	2.28	1.98	2.03	2.34
Cu−O	2.01	2.06[a]	2.13	1.93	2.07	2.36
Cu−S	2.40	2.49	2.41	2.28	2.43	2.72

[a] A value of 2.16 is obtained when the (**5d-5**) structure is considered as a regular 5-coordinated complex.

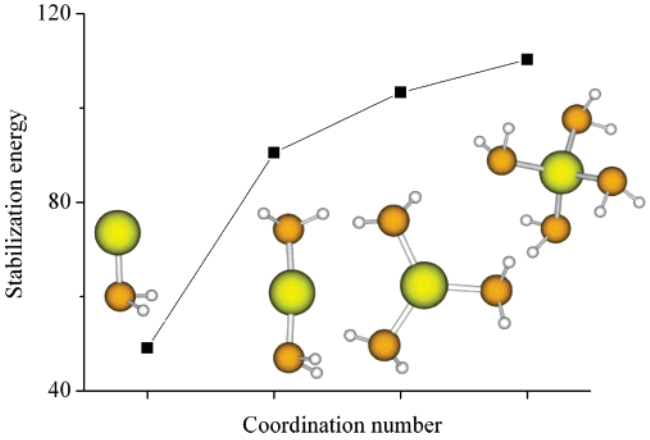

Figure 6. Dependence of stabilization energy (ΔE^{stab}) on the number of coordinated sulfide molecules in the Cu(I) compounds.

electrostatic repulsion of the H_2S molecules is relatively small due to a small dipole moment, a lower coordination leads to less stable systems. Also, electrostatic repulsion in the case of a larger number of ligands is reduced as a consequence of longer metal−ligand distances. This situation can be demonstrated on the structure (**1d-3**) where the three first-shell H_2S ligands contribute to the total stabilization by 34.3 kcal/mol each (from a ΔE^{coord} value of 102.9 kcal/mol), while the remaining H_2S molecule outside the first shell is attracted to the complex (H-bonding to the first-shell H_2S + electrostatic interaction with Cu^+) by only 5.7 kcal/mol, resulting in a final ΔE^{stab} value of 108.6 kcal/mol.

In the case of $[Cu(H_2S)_6]^{2+}$, a slightly larger donation from 5-coordinated ligands (**2f-5**) than from 4-coordinated ligands (**2f-4**) was found. The difference in the ΔE^{stex} values is about 1 kcal/mol. Larger ΔE^{stex} energy values are compensated by

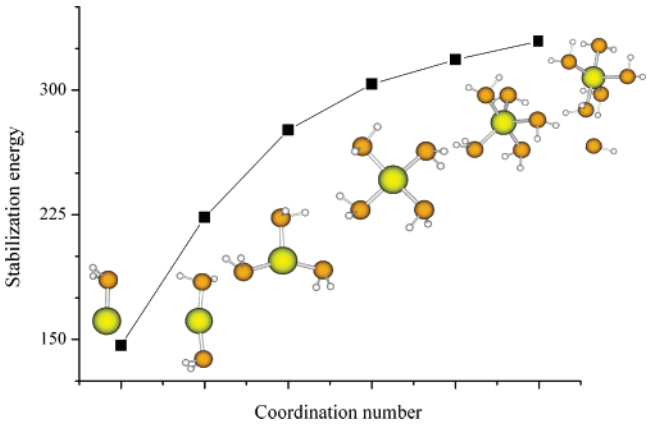

Figure 7. Dependence of stabilization energies (ΔE^{stab}) on the coordination number of the H_2S molecules in the $[Cu(H_2S)_n]^{2+}$ complexes ($n = 1-6$).

TABLE 5: ΔE^{stab} Stabilization Energies (in kcal/mol), the 4s AO Occupations, and the Partial Charges (in *e*) on the Cu Atom for Mixed Cu(I) Systems[a]

system	struct	ΔE^{stab}	δ(Cu)	4s
$[Cu(H_2S)_4]^+$	**3a-3**	108.6	0.61	0.45
	3a-4	*110.3*	*0.60*	*0.43*
$[Cu(H_2S)_2(H_2O)_2]^+$	**3b-2**	112.1	0.67	0.54
	3b-3	*116.6*	*0.70*	*0.37*
	3b-4	112.2	0.73	0.34
$[Cu(H_2S)_2(H_2O)(NH_3)]^+$	**3c-2**	121.7	0.62	0.53
	3c-3	*123.8*	*0.67*	*0.41*
	3c-4	121.4	0.71	0.36
$[Cu(H_2S)_2(NH_3)_2]^+$	***3d-2***	*130.5*	*0.67*	*0.54*
	3d-3	127.1	0.73	0.36
	3d-4	126.6	0.73	0.33
$[Cu(H_2O)_4]^+$	***3e-2***	*117.6*	*0.80*	*0.41*
	3e-3	112.0	0.87	0.24
	3e-4	106.7	0.88	0.19
$[Cu(H_2O)_2(NH_3)_2]^+$	***3f-2***	*139.8*	*0.66*	*0.55*
	3f-3	138.1	0.73	0.44
$[Cu(NH_3)_4]^+$	***3g-2***	*144.4*	*0.65*	*0.56*
	3g-3	140.5	0.76	0.34
	3g-4	139.3	0.80	0.24

[a] Italic font indicates the global minima. The abbreviation struct is used for exact identification of the optimized structure.

larger ligand repulsion, giving the same ΔE^{stab} stabilization energy. A similar situation occurs also in the $[Cu(H_2S)_5]^{2+}$ complexes, where the final preference for the 5-coordinated structure is slightly more distinct. A ligand repulsion can be evaluated from differences between corresponding ΔE^{stab} and ΔE^{stex} values (see method). These differences are up to 18 kcal/mol for 5-coordinated complexes.

Table 5 collects the ΔE^{stab} stabilization energies for the monovalent copper cation in a mixed ligand environment. It was found that 2-coordination is preferred in complexes with at least two ammine ligands or more than two aqua ligands. Other mixed systems prefer the 3-coordinated structures as the most stable and only the tetrasulfide complex has the highest stabilization in a 4-coordinated arrangement. Comparing 4-coordinated complexes, $[Cu(NH_3)_4]^+$ is the most stable complex with ΔE^{stab} values equal to 139 kcal/mol. $[Cu(H_2S)_4]^+$ displays about 30 kcal/mol lower of a stabilization energy. The 4-coordinated $[Cu(H_2O)_4]^+$ is the least stable complex. However, the 4-coordinated $[Cu(H_2O)_4]^+$ structure does not represent the most stable structure analogously to the tetraamine compounds. For example, the 3-coordinated $[Cu(H_2O)_4]^+$ complex has larger stabilization than any $[Cu(H_2S)_4]^+$ system. The higher stability is connected with a relatively strong H-bond of the water

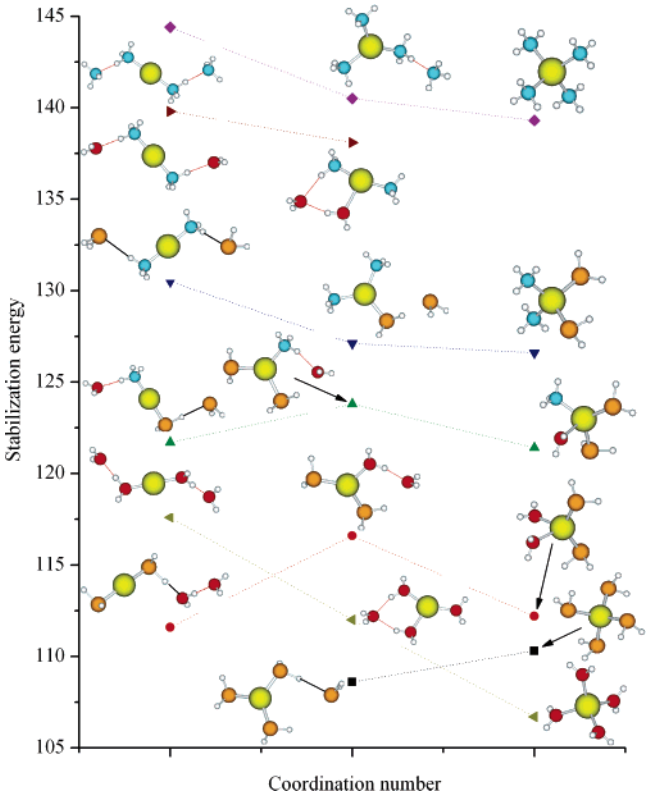

Figure 8. Stabilization energies (ΔE^{stab}) for the mixed $[Cu(H_2S)_m(H_2O)_n(NH_3)_k]^+$ compounds ($n + m + k = 4$): (▼) $[Cu(H_2S)_2(NH_3)2]^{2+}$; (▲) $[Cu(H_2S)_2(H_2O)(NH_3)]^{2+}$; (●) $[Cu(H_2S)_2(H_2O)_2]^{2+}$; (■) $[Cu(H_2S)_4]^{2+}$; (right-pointing triangle) $[Cu(H_2O)_4]^{2+}$; (left-pointing triangle) $[Cu(H_2O)_2(NH_3)_2]^{2+}$; (◆) $[Cu(NH_3)_4]^{2+}$.

molecule in the second solvation shell which masks the correct binding trend. This trend can be recovered from the coordination energies. The ΔE^{coord} value of the Cu−S bond is about 31.3 kcal/mol (from Table 1). It is practically identical to the corresponding value for the Cu−O bond (31.1 kcal/mol), published earlier.[65]

The preference order of the ΔE^{stab} energies, $Cu^+-N > Cu^+-S \geq Cu^+-O$, can be observed also for other systems in Table 5. Figure 8 helps to highlight the obtained trends. For instance, the most stable conformer of the $[Cu(H_2S)_2(H_2O)_2]^+$ system forms two Cu−S bonds while expelling the water molecules to the second solvation shell. The inverted conformer with two aqua ligands and two sulfide molecules in the second shell possesses about 6.6 kcal/mol lower stabilization energy.

Comparing the ΔE^{stab} values in a series of 4-coordinated $[Cu(H_2S)_2(X)_2]^+$ complexes (X = NH_3, H_2O, H_2S), the higher stabilization of the diaqua complex seemingly violates the overall trend. However, less bulky ligands (NH_3 or H_2O) allow shorter Cu−S distances, that is, larger overlap and stronger dative bonds, which leads to better stabilization of the mixed 4-coordinated $[Cu(H_2S)_2(H_2O)_2]^+$ complex. This is also supported by the bonding energies (see the upper part of Table 7). The disulfide−diaqua system possesses the largest ΔE^{BE} values for the Cu−S bonds in all Cu(I) complexes. Moreover, a small O−Cu−O angle (80°) and a HO−H···OH_2 distance of 2.6 Å clearly point to an additional interligand H-bond stabilization.

Stabilization energies for Cu(II) complexes are collected in Table 6. In the upper part of Table 6, the ΔE^{stab} and ΔE^{stex} energies of 4-coordinated Cu(II) complexes exhibit one important difference in comparison with the Cu(I) systems. The order of binding preference changes to Cu−N > Cu−O ≥ Cu−S. This is due to a larger electrostatic contribution to the metal−ligand bond. The stabilization energy of $[Cu(H_2O)_4]^{2+}$ is comparable to the ΔE^{stab} value of $[Cu(H_2S)_2(H_2O)_2]^{2+}$ and is about 3 kcal/mol higher than that of $[Cu(H_2S)_4]^{2+}$. The differences become more distinct when sterical corrections and H-bonding interactions are omitted, as was found for the ΔE^{stex} values.

In the lowest part of Table 6, the complexes with six interacting molecules are collected. Three different coordinations were examined. In all cases, 4-coordinated structures represent the most stable complexes. Nevertheless, sometimes (e.g., $[Cu(H_2S)_6]^{2+}$ or $[Cu(NH_3)_6]^{2+}$), the stabilization of 5-coordinated complexes is quite comparable (structures **5a-5** and **5c-5**). Moreover, the ΔE^{stex} energies, which evaluate the pure Cu/ligands interaction, are larger for 5-coordinated structures in all three homoligated systems. The largest interligand repulsion occurs in the case of 5-coordinated $[Cu(H_2S)_2(NH_3)_4]^{2+}$, where four ammine ligands occupy the first solvation shell. Figure 9 illustrates the dependence of the stabilization energy on the composition of these Cu(II) complexes. The strongest Cu−N bonding energies and larger stabilization energies in ammine-containing complexes are clearly demonstrated.

3.3. Ligand Bonding Energy (BE). The ΔE^{BE} energies of all Cu−X bonds (X = NH_3, H_2O, and H_2S) are presented in the upper part of Table 7 for the 4-coordinated Cu(I) complexes. Partition of the complex into two parts (ligand and the remaining part of the complex) in eq 1 enables a deeper insight into the strength of the individual Cu−X bonds. The ΔE^{BE} energies reflect closely the copper−ligand distances. In agreement with previous observations, the largest values in homoligated complexes (**3a-4**, **3e-4**, and **3g-4**) were found for the Cu−N bonds (about 21.1 kcal/mol). They are followed by an average ΔE^{BE} value of 17.7 kcal/mol for Cu−O and 15.6 kcal/mol for Cu−S. The strongest Cu−N bond occurs in the mixed $[Cu(H_2S)_2(H_2O)(NH_3)]^+$ complex characterized by about 29.9 kcal/mol. In this complex, the donation competition from the other ligands is relatively weak. The inconsistency in $(\Delta E^{BE}([Cu(H_2O)_4]^+) - \Delta E^{BE}([Cu(H_2S)_4]^+))$ versus $(\Delta E^{stab}([Cu(H_2O)_4]^+) - \Delta E^{stab}([Cu(H_2S)_4]^+))$ energies can be explained by stronger (repulsive) dipole/dipole interaction of water molecules, which lowers the stabilization energy of the tetraaqua complexes.

The ΔE^{BE} energies for the $[Cu(ligand)_4]^{2+}$ complexes are listed in the second part of Table 7. Similar to the Cu(I) systems, the relation between the BE values and the Cu−X distances (X = NH_3, H_2O, and H_2S) was found. Surprisingly, for the pure tetraamine, tetraaqua, and tetrasulfide complexes, very similar BEs for Cu−N and Cu−O were obtained (49.9 and 49.6 kcal/mol, respectively). The BE value of Cu−S is substantially smaller (34.8 kcal/mol). In accordance with the suggested stabilization order, an analogous preference of BE can be noticed. In the mixed Cu(II) systems, dependence of the ΔE^{BE} energies on various Cu−X bonds is more complex. An interesting situation occurs in the $[Cu(H_2S)_2(NH_3)_2]^{2+}$ system, where the ΔE^{BE}'s of Cu−N are not as high as those in the $[Cu(H_2O)_2(NH_3)_2]^{2+}$ complex. Similarly, the smallest value of Cu−S can also be seen in the $[Cu(H_2S)_2(NH_3)_2]^{2+}$ complex. This can be explained by different conformations. While the global minimum is the trans conformer in $[Cu(H_2S)_2(NH_3)_2]^{2+}$, all remaining 4-coordinated complexes prefer cis conformers as the most stable arrangements. The trans effect leads to the largest BE values for the Cu−N bond in the *cis*-$[Cu(H_2O)_2(NH_3)_2]^{2+}$ complex. This effect also results in lower BE values of the Cu−O bond in comparison with the tetraaqua complex (by about 10 kcal/mol). Simultaneously, the BE of Cu−N is

TABLE 6: Stabilization ΔE^{stab} and Sterically Corrected Stabilization ΔE^{stex} Energies (in kcal/mol), Partial Charges δ(Cu), Spin Densities ρ_S(Cu), and 4s and 3d Occupations of the Copper AO (in *e*) for the Cu(II) Systems[a]

system	struct	ΔE^{stab}	ΔE^{stex}	δ(Cu)	ρ_S(Cu)	4s	3d
$[Cu(H_2S)_4]^{2+}$	**4a**	303.6	313.9	0.87	0.40	0.53	9.56
$[Cu(H_2S)_2(H_2O)_2]^{2+}$	**4b**	306.4	316.7	1.12	0.54	0.44	9.41
$[Cu(H_2S)_2(H_2O)(NH_3)]^{2+}$	**4c**	321.1	334.4	1.13	0.54	0.42	9.42
$[Cu(H_2S)_2(NH_3)_2]^{2+}$	**4d**	335.3	349.6	1.16	0.53	0.39	9.41
$[Cu(H_2O)_4]^{2+}$	**4e**	306.9	321.1	1.56	0.77	0.24	9.18
$[Cu(H_2O)_2(NH_3)_2]^{2+}$	**4f**	340.2	359.5	1.40	0.68	0.31	9.27
$[Cu(NH_3)_4]^{2+}$	**4g**	366.8	391.8	1.30	0.63	0.36	9.32
$[Cu(H_2S)_6]^{2+}$	**5a-4**	329.4	346.3	0.86	0.38	0.52	9.58
	5a-5	*329.4*	*347.2*	*0.86*	*0.40*	*0.53*	*9.56*
$[Cu(H_2O)_6]^{2+}$	***5b-4***	*363.4*	*376.4*	*1.24*	*0.74*	*0.26*	*9.21*
	5b-5	358.6	377.1	1.22	0.79	0.24	9.18
	5b-6	338.0	362.2	1.43	0.88	0.24	9.10
$[Cu(NH_3)_6]^{2+}$	***5c-4***	*407.5*	*437.7*	*1.38*	*0.60*	*0.37*	*9.34*
	5c-5	407.1	444.6	1.32	0.66	0.34	9.30
	5c-6	399.9	443.7	1.30	0.68	0.34	9.28
$[Cu(H_2S)_2(H_2O)_4]^{2+}$	***5d-4***	*356.7*	*370.4*	*1.19*	*0.56*	*0.39*	*9.39*
	5d-5	351.7	368.1	1.24	0.60	0.36	9.36
	5d-6	343.7	364.2	1.28	0.65	0.35	9.33
$[Cu(H_2S)_4(H_2O)_2]^{2+}$	***5e-4***	*342.9*	*359.2*	*0.86*	*0.56*	*0.53*	*9.56*
	5e-5	342.5	356.7	0.95	0.60	0.48	9.53
	5e-6	336.0	355.0	0.98	0.46	0.46	9.51
$[Cu(H_2S)_2(H_2O)_2(NH_3)_2]^{2+}$	***5f-4***	*376.0*	*397.1*	*1.26*	*0.60*	*0.38*	*9.34*
	5f-5	375.0	396.5	1.23	0.61	0.39	9.34
	5f-6	368.9	394.4	1.20	0.58	0.39	9.37
$[Cu(H_2S)_2(NH_3)_4]^{2+}$	***5g-4***	*389.0*	*421.4*	*1.28*	*0.60*	*0.37*	*9.34*
	5g-5	387.6	420.5	1.29	0.63	0.37	9.32
$[Cu(H_2S)_4(NH_3)_2]^{2+}$	**5h-4**	359.6	*385.5*	1.09	0.50	0.44	9.43
	5h-5	*360.3*	384.7	*1.10*	*0.54*	*0.45*	*9.41*

[a] The abbreviation struct is used for exact identification of the optimized structure. Italic font indicates the global minima.

TABLE 7: Bonding Energies ΔE^{BE} (in kcal/mol) for the 4-Coordinated Cu(I) and Cu(II) Complexes[a]

system	struct	Cu−X1	Cu−X2	Cu−X3	Cu−X4
$[Cu(H_2S)_4]^{+}$	**3a-4**	15.6*	15.6*	15.6*	15.6*
$[Cu(H_2S)_2(H_2O)_2]^{+}$	**3b-4**	22.9*	22.1*	14.0**	12.5**
$[Cu(H_2S)_2(H_2O)(NH_3)]^{+}$	**3c-4**	29.9	18.8*	18.6*	9.5**
$[Cu(H_2S)_2(NH_3)_2]^{+}$	**3d-4**	23.3	22.5	13.0*	12.6*
$[Cu(H_2O)_4]^{+}$	**3e-4**	24.8**	18.1**	14.6**	13.4**
$[Cu(NH_3)_4]^{+}$	**3g-4**	21.1	21.1	21.1	21.1
$[Cu(H_2S)_4]^{2+}$	**4a**	35.3*	34.8*	34.5*	34.4*
$[Cu(H_2S)_2(H_2O)_2]^{2+}$	**4b**	46.8*	46.1*	38.0**	37.0**
$[Cu(H_2S)_2(H_2O)(NH_3)]^{2+}$	**4c**	55.5	40.9*	40.2*	32.7**
$[Cu(H_2S)_2(NH_3)_2]^{2+}$	**4d**	54.9	54.7	31.2*	30.9*
$[Cu(H_2O)_4]^{2+}$	**4e**	49.6**	49.6**	49.6**	49.6**
$[Cu(H_2O)_2(NH_3)_2]^{2+}$	**4f**	62.9	62.9	39.2**	39.2**
$[Cu(NH_3)_4]^{2+}$	**4g**	49.9	49.9	49.9	49.9

[a] The abbreviation struct is used for exact identification of the optimized structure. One asterisk denotes Cu−S bond lengths, and two asterisks denote Cu−O bond lengths, while all remaining values are those for Cu−N bonds.

increased by a similar amount of energy as compared to the tetraammine complex. Also, in the $[Cu(H_2S)_2(H_2O)_2]^{2+}$ complex, similar BE shifts can be observed. The ΔE^{BE} values of the Cu−S and Cu−O bonds respectively are larger by about 10 kcal/mol and smaller by about the same amount than the ΔE^{BE} energies in the corresponding homoligated complexes. Moreover, in the $[Cu(H_2S)_2(H_2O)_2]^{2+}$ and $[Cu(H_2S)_2(H_2O)(NH_3)]^{2+}$ complexes, the Cu−S bonds are characterized by larger ΔE^{BE} values than the Cu−O bonds. This is caused by a larger donation contribution in the Cu−S bonds, which can be demonstrated in the framework of the natural bond orbital (NBO) analysis. The donation of a lone pair of the sulfur atom to the first virtual orbital of Cu can be evaluated in terms of the *E*(2) energies (the second-order perturbation theory of the Fock matrix in the basis of NBO) to be about 40 kcal/mol. The same *E*(2) energies from the lone pairs of oxygen atoms are lower by about 20 kcal/mol. In the case of the $[Cu(H_2S)_2(H_2O)(NH_3)]^{2+}$ complexes, a similar situation was obtained. The *E*(2) energies are the following: *E*(2)(O→Cu) ≈ 15 kcal/mol, *E*(2)(N→Cu) ≈ 30 kcal/mol, and *E*(2)(S→Cu) ≈ 40 kcal/mol.

3.4. IPs and EAs. To describe transitions between Cu(I) and Cu(II) oxidation states, the vertical and adiabatic ionization potentials were calculated. In the case of IP_{vert}, both HF and DFT levels were considered. In the case of IP_{adiab}, only the DFT method was used. The IP values are compiled in Table 8.

At the DFT level, the IP_{vert} values decrease with increasing coordination number. In 4-coordinated systems, the highest values (12.0−12.7 eV) were obtained for the sulfide-containing complexes. Slightly lower IPs were obtained for the tetraaqua and tetraamine complexes (11.9 and 11.3 eV, respectively). The IP_{adiab} values are lower by approximately 0.5 eV. Interestingly, for the $[Cu(H_2O)_4]^{2+/+}$ system, practically the same vertical and adiabatic IPs were obtained. From the difference between IP values, one can estimate the relaxation strain, which pushes the instantly oxidized Cu(I) structure toward the optimal Cu(II) geometry. In the case of the tetraaqua complex, this points to a very flat potential energy surface in relation to the deformation of torsion angles. In blue copper proteins, the ligand arrangement of the active center usually has a distorted tetrahedral structure, which is probably also enforced for the Cu(II) structure. This fact partially explains their large reduction potential. The $[Cu(H_2S)_2(NH_3)_2]^{+}$ complex can be of particular interest, since its IPs might give insight into the redox center of proteins such as plastocyanin or azurin. They contain two histidines, one methionine, and cysteine amino acid side chains coordinated to the copper cation. In the $[Cu(H_2S)_2(NH_3)_2]^{+}$ complex, the IP_{vert} value is equal to 12.0 eV and IP_{adiab} = 11.5 eV. Unfortunately, we are not aware of any experimental data for these small complexes that could be compared with the presented results. Nevertheless, theoretical papers presenting the ionization potentials for similar compounds exist. In the study of Taylor,[87] vertical IP = 6.27 eV was calculated for the neutral $Cu(H_2O)$ molecule at the CCSD(T) level. The values of the

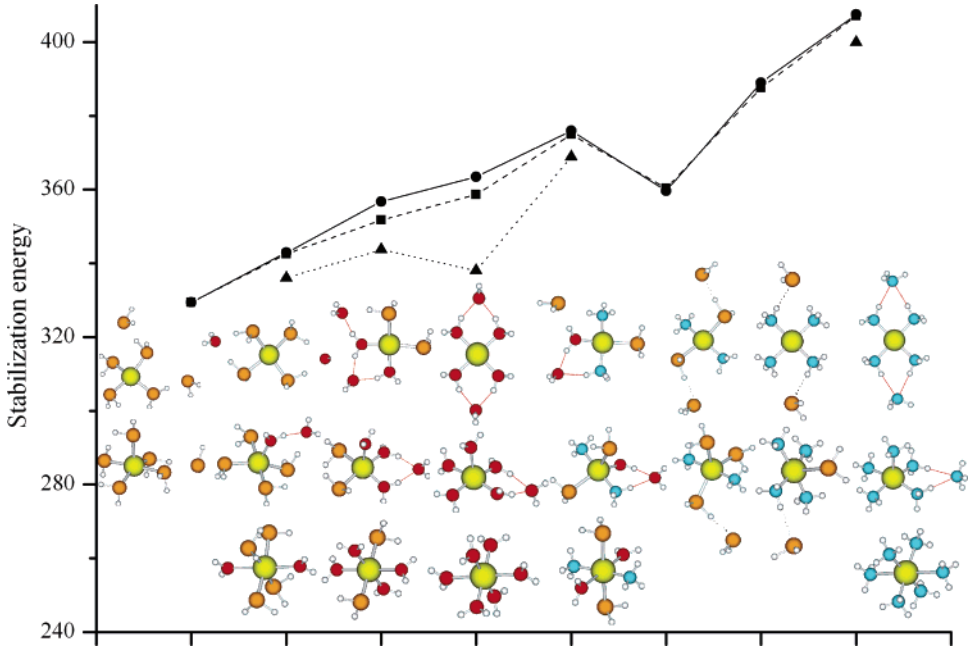

Figure 9. Dependence of stabilization energy on the coordination number of the Cu(II) complexes: (●) 4-coordinated, (■) 5-coordinated, and (▲) 6-coordinated structures.

TABLE 8: Ionization Potentials (in eV) IP_{vert}, IP_{adiab}, IP_{Koop}, and IP_{OVGF} and Electron Affinities EA_{vert} and EA_{OVGF} for the Cu(I) Complexes[a]

system	struct	IP_{vert} DFT	IP_{adiab} DFT	IP_{Koop} DFT	IP_{vert} HF	IP_{Koop} HF	IP_{OVGF} HF	EA_{vert} DFT	EA_{OVGF} HF
$[Cu(H_2S)_4]^+$	**3a-3**	12.6		10.8	13.6	13.8	13.2	3.5	2.9
	3a-4	*12.6*	*12.2*	*10.7*	*13.2*	*14.5*	*14.9*	*3.5*[b]	*2.9*
$[Cu(H_2S)_2(H_2O)_2]^+$	**3b-2**	13.6		11.4	14.5	15.1	16.3	3.3	2.7
	3b-3	13.0		10.8	13.7	14.8	15.5	3.5	2.7
	3b-4	*12.7*	*12.1*	*10.6*	*13.6*	*14.6*	*15.4*	*3.5*	*2.9*
$[Cu(H_2S)_2(H_2O)(NH_3)]^+$	**3c-2**	12.9		10.8	14.6	13.8	13.1	3.3	2.6
	3c-3	12.5		10.5	13.4	14.3	15.2	3.4	2.7
	3c-4	*12.4*	*11.9*	*10.4*	*13.3*	*14.3*	*15.2*	*3.4*	*2.8*
$[Cu(H_2S)_2(NH_3)_2]^+$	**3d-2**	12.4		10.7	12.4	13.8	13.1	3.3	2.5
	3d-3	12.1		10.2	12.2	13.6	13.0	3.4	2.8
	3d-4	*12.0*	*11.5*	*10.0*	*12.9*	*13.9*	*14.8*	*3.4*	*2.8*
$[Cu(H_2O)_4]^+$	**3e-2**	13.7		10.9	15.2	15.5	79.8	3.5	2.4
	3e-3	13.0		10.1	15.1	15.5	36.9	3.7	2.8
	3e-4	*11.9*	*11.9*	*10.0*	*15.2*	*14.0*	*27.9*	*2.9*	*2.8*
$[Cu(H_2O)_2(NH_3)_2]^+$	**3f-2**	13.2		10.6	14.5	14.8		3.2	2.9
	3f-3	*12.5*	*11.8*	*9.9*	*15.6*	*14.4*	*34.4*	*3.3*	*2.4*
$[Cu(NH_3)_4]^+$	**3g-2**	12.8		10.5	10.0	14.6	36.0	3.0	2.7
	3g-3	11.9		9.4	12.9	14.5	26.7	3.2	2.6
	3g-4	*11.3*	*10.7*	*8.8*	*13.8*	*14.0*	*47.4*	*3.3*	*2.6*

[a] Italic font indicates transitions between the 4-coordinated structures. The abbreviation struct is used for the optimized structure. [b] The adiabatic EA of the $[Cu(H_2S)_4]^+$ complex is 3.5 eV. The neutral structure of 4-coordinated $[Cu(H_2S)_4]$ has a tetrahedral geometry with Cu−S distances of ∼2.38 Å.

vertical and adiabatic IPs of phthalocyanine were determined to be 6.48 and 6.47 eV, respectively, by Lee[88] using the BPW91 method. Olsson[10] calculated the vertical QM/MM energy difference of the two states in the presence of protein point charges and obtained 4.22 and 6.78 eV for plastocyanin and rusticyanin, respectively. Our results can be compared with the vertical IPs of Satta et al.[89] who investigate neutral $Cu(NH_3)_n$ systems at the B3LYP level. They found vertical IP = 3.70, 3.65, and 2.90 eV for n = 2, 3, and 4, respectively. Our estimation of the EA value for $[Cu(NH_3)_4]^+$ is 3.3 eV, which is in good accord with the energy computed by Satta.

For the Cu(I) systems, the IP_{Koop} ionization potentials based on Koopmans' theorem are presented as well. These values are systematically about 2 eV lower at the DFT level and about 1 eV higher at the HF level than the corresponding IP_{vert} energies. Comparing the IP_{vert} energies obtained at the HF and DFT levels, one can see that the DFT values are generally lower.

An estimation of the adiabatic electron affinity was performed. However, the only stable neutral structure was found for the 4-coordinated $[Cu(H_2S)_4]$ system. The calculated adiabatic electron affinity is about 3.5 eV. The additional electron is located in the LUMO of the Cu(I) structures that is composed by the copper 4s atomic orbital (AO) with an antibonding admixture of sulfide MOs. The vertical EA_{vert}(DFT) electron affinity values were evaluated for all studied Cu(I) complexes. They range from 2.9 to 3.7 eV.

Results from outer valence Green function propagators systematically overestimate IPs (even more than 2.0 eV) and underestimate EAs (on average by 0.5 eV). Also, the trend in IP^{OVGF} is not correct, since the IP increases with increasing coordination.

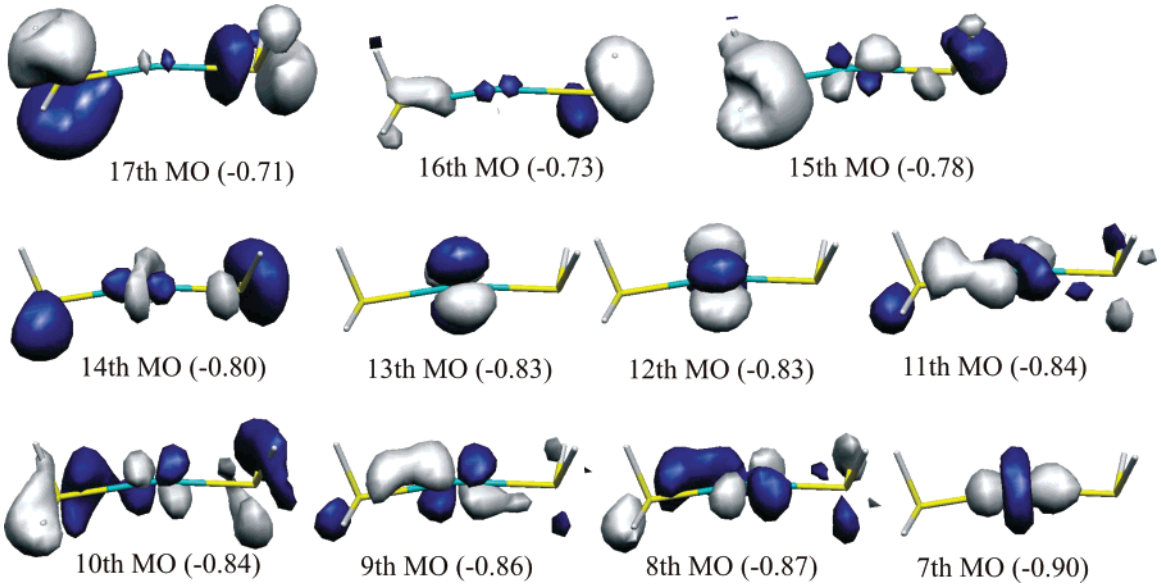

Figure 10. Valence α-MOs of the $[Cu(H_2S)_2]^{2+}$ system. The orbital energies of the corresponding MOs are in parentheses (in au). The 11th α-MO (SOMO) has no corresponding MO in the β-set.

For an accuracy estimation, the experimentally measured first and second ionization potentials and the EA of the isolated Cu atom ($IP^{first} = 7.7$ eV, $IP^{second} = 20.3$ eV, EA = 1.2 eV[90]) were compared with the calculated values ($IP^{first} = 8.2$ eV, $IP^{second} = 20.5$ eV, EA = 1.3 eV). Relatively similar values at least partially justify the methods and basis set used in this section.

3.5. Charge and Wave Function Analyses. The partial charges were determined by the NPA method,[76] and an analysis of molecular orbitals (MOs) was performed in order to get a deeper insight into the interactions in the examined structures. The Cu(II) complexes contain copper in the $3d^9$ configuration, giving an open-shell wave function with the doublet electronic ground state. According to the arrangement of ligand molecules in the first solvation shell, the single occupied molecular orbital (SOMO) is formed by different Cu 3d atomic orbitals (AOs). In the $[Cu(H_2S)]^{2+}$ and $[Cu(H_2S)_2]^{2+}$ structures, the SOMO is composed of the $3d_{z^2}$ AO (11th MO in Figure 10) with the z-axis collinear to the copper−ligand bond. In the most stable square-planar 4-coordinated complexes, the $3d_{x^2-y^2}$ AO of the Cu atom forms the SOMO. This can be observed in Figure 11 and Supporting Information Figures 1 and 2. For the 5- and 6-coordinated structures, the SOMOs are also based on the $3d_{x^2-y^2}$ AO with partial admixture of Cu $3d_{z^2}$.

Table 1 contains the copper partial charges for all studied copper sulfide compounds. In both monovalent and divalent cations, the Cu 4s AO plays a key role in donation effects. Occupations of this orbital (and 3d AOs in the case of the Cu(II) systems) are also presented in Table 1. Increasing coordination number leads to the saturation of the acceptor ability of the Cu ions. In the case of three or more ligands, no substantial change of the Cu partial charge occurs (about 0.6 and 0.9*e* in the monovalent and divalent complexes, respectively). The value of the metal partial charge results from the extent of the ligand electron-density donation, which is a consequence of the chemical potential minimization of the whole system. Also, the spin density localized on the Cu atom closely follows the size of partial charge, as can be seen from Table 1 for homoligated structures and Table 6 for mixed ligand complexes. An interesting exception from this correspondence between partial charges and spin densities is the system $[Cu(H_2S)_2]^{2+}$ where a relatively high spin density on the Cu atom can be noticed. A possible explanation comes from the different donation in the case of the monosulfide $[Cu(H_2S)]^{2+}$ complex where the main dative contribution to 3d can be noticed (9.58*e*). In the disulfide complex, practically the same donation to the 4s Cu AO is visible (0.39) comparing to 9.39*e* in 3d AOs. It means that the smaller portion of the α-spin electron density from $3d_{x^2-y^2}$ is compensated in this complex. When more than two ligands are present, the accepting capability of the Cu^{2+} cation is already saturated as follows from the nearly constant occupation of both the 3d (≈9.56*e*) and 4s (≈0.53*e*) AOs of the Cu atom. The donation to different types of Cu AOs for mono- and di-ligated complexes is general, and it also was observed in the previous studies with water[65] and ammonia[66] ligands. Here, a different target (different AO of Cu) caused stronger and shorter Cu−O and Cu−N bonds (or higher stabilization) in diaqua or diammine complexes than it would correspond to monotonic trends when number of ligands was increased.

The NPA partial charges of the monovalent Cu complexes in a mixed sulfide−water−ammonium environment are compiled in Table 5. In the Cu(I) water−ammonium compounds, the highest donation and thus the lowest Cu partial charge occurs in 2-coordinated structures. In the presence of hydrogen sulfide molecules, lower partial charges on the Cu cations point to a higher donation. This observation is in agreement with the coordination preferences found in the energy section above. The same dependence of the partial charges on the ligand type can also be found in the mixed Cu(II) systems in Table 6. These trends correspond to increasing values of hardness, $\mu(H_2S) = 6.2$, $\mu(NH_3) = 8.2$, $\mu(H_2O) = 9.5$,[91] and reflect the principle of the HSAB theory.[82]

Detailed insight into the donor−acceptor bonding character can be achieved by molecular orbital (MO) analysis. For the demonstration, 2-coordinated $[Cu(H_2S)_2]^{2+}$ (in Figure 10) and 4-coordinated homoligated complexes were chosen. Several highest valence MOs are depicted for the tetrasulfide complex in Figure 11. Supporting Information Figure 1 shows valence MOs for the tetraammine Cu(II) structure, and MOs of the tetraaqua Cu(II) complexes are depicted in Supporting Information Figure 2. In 4-coordinated complexes, the proper $d_{x^2-y^2}$ character of the SOMO (13th MO in Figure 11, 21st MO in Supporting Information Figure 1, and 17th MO in Supporting Information Figure 2) can be seen. The lower occupation of

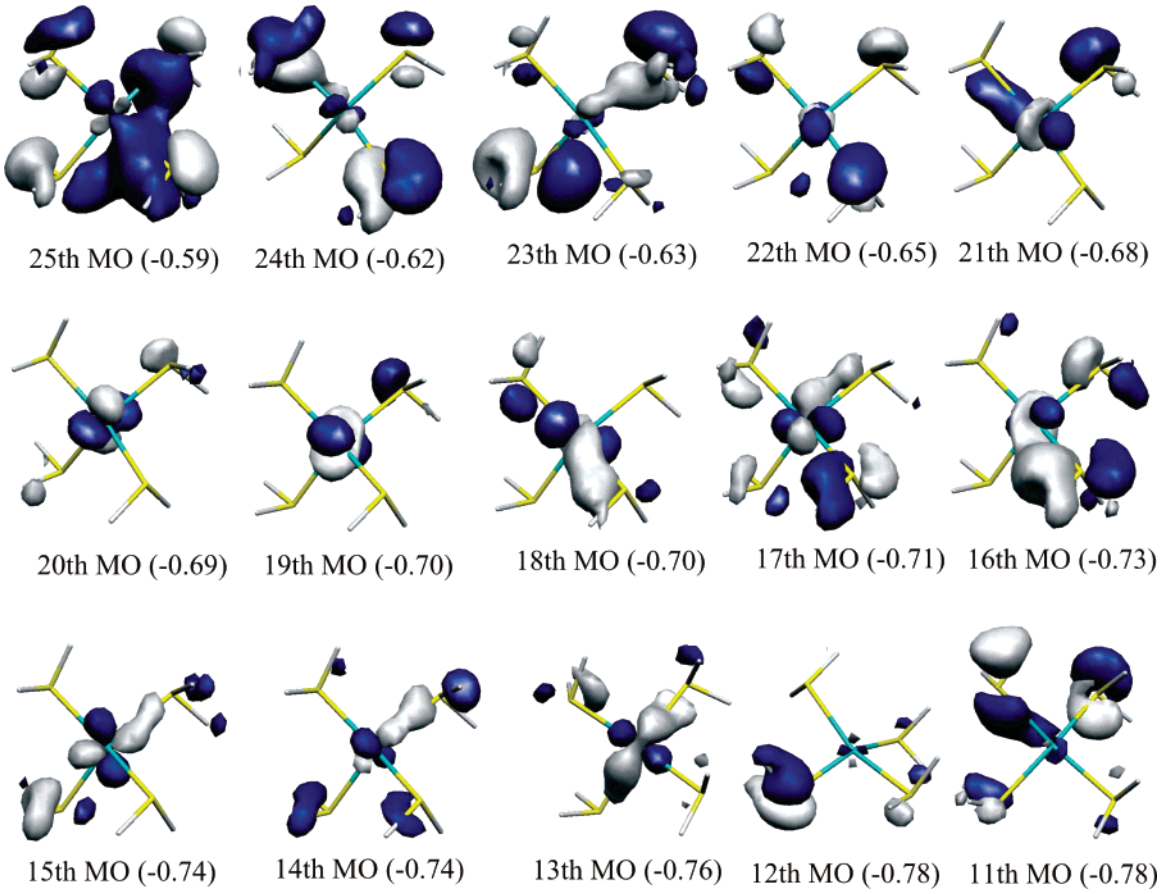

Figure 11. Valence α-MOs of the $[Cu(H_2S)_4]^{2+}$ system. The SOMO is represented by the 13th MO.

the $3d_{x^2-y^2}$ AO minimizes the repulsion between the Cu electron density and the donating ligand lone pairs. The varying "position" of the SOMO orbital is connected with the different eigenvalues of the MOs in isolated ligand molecules and with the usage of an unrestricted method. In Figure 11, the first three MOs (23rd to 25th) display the nonbonding combinations of lone pairs of the H_2S ligands (with small admixture of Cu AOs $3d_{x^2-y^2}$, $3d_{xz}$, and $3d_{yz}$ according to the symmetry of the ligands). In the four following orbitals, the Cu 3d AOs dominate (19th to 22nd): d_{z^2}, d_{xy}, d_{xz}, d_{yz}. Then, another set of five MOs appears where only a small contribution of the Cu d AO is admixtured to ligand MOs. Finally, the 13th α-orbital with $d_{x^2-y^2}$ character appears, which has no similar counterpart among the occupied β-orbitals. An analogous discussion applies also to the remaining two cases. No back-donation strengthening of the Cu−X bonds can occur in the examined complexes, since none of the examined ligands possess proper π^*-antibonding orbitals.

In the first column of Figure 12, the spin densities (on the isodensity surface of $\rho = 0.005$ e/bohr^3) for linear disulfide, square-planar tetraaqua, tetraamine, and tetrasulfide Cu(II) complexes are depicted. Except for the first linear one, all of the other densities show the same shape in which the character of the copper $3d_{x^2-y^2}$ AO can be easily recognized. The second column of Figure 12 presents maps of electrostatic potentials projected on the isodensity surface ($\rho = 0.001$). A higher maximum of the electrostatic potential (V_{max}) in the case of the tetraaqua complex corresponds to a relatively smaller donation in accord with the NPA partial charges.

Using the MP2/6-31+G(d) method, Katz et al.[18] determined partial charges of 0.71 and 1.38*e* on the Cu atom in the $[Cu(H_2S)_4]^+$ and $[Cu(H_2S)_4]^{2+}$ systems, respectively. However, the present values for the Cu(I) and Cu(II) structures are substantially lower (0.4 and 0.8*e*, respectively) using a larger basis set (B3LYP/6-311++G(2df,2pd)). For the $[Cu(NH_3)_4]^{2+/+}$ complexes, similar (but not so significant) differences between the MP2/6-31+G(d) and B3LYP/6-311++G(2df,2pd) results can be noticed (1.3 and 1.6*e* compared with 0.8 and 0.87*e* for Cu(I) and Cu(II), respectively). An explanation of the remarkably higher Cu partial charges can be seen in inaccurate description of sulfur-containing systems using the MP2 method (cf. ref 92) and a slightly less flexible (smaller) basis set in the case of Katz's calculation.

4. Conclusion

A systematic investigation of the Cu(I)/Cu(II) cation interactions with biologically important types of ligands (water, ammonium, and hydrogen sulfide) at the DFT level was performed. The $[Cu(H_2S)_m(H_2O)_n(NH_3)_k]^{2+}$ complexes (where *n*, *m*, and *k* are equal to 0, 2, 4, and 6, along with the restriction $m + n + k = 4$ or 6) were optimized using the B3PW91/6-31G(d) method, often using distinct geometries as starting points. In the case of the Cu(I) complexes, only the 4-ligated systems ($m + n + k = 4$) were examined, since a maximum coordination number of 4 was reported in previous studies. The optimizations reveal various stable coordinations.

The lowest conformers of all coordinations were analyzed in terms of the ΔE^{stab} and ΔE^{stex} stabilization energies, ΔE^{coord} coordination energies and ΔE^{BE} bonding energies at the B3LYP/6-311++G(2df,2pd) level. The different schemes to describe the energetics help one to better understand the balance of forces

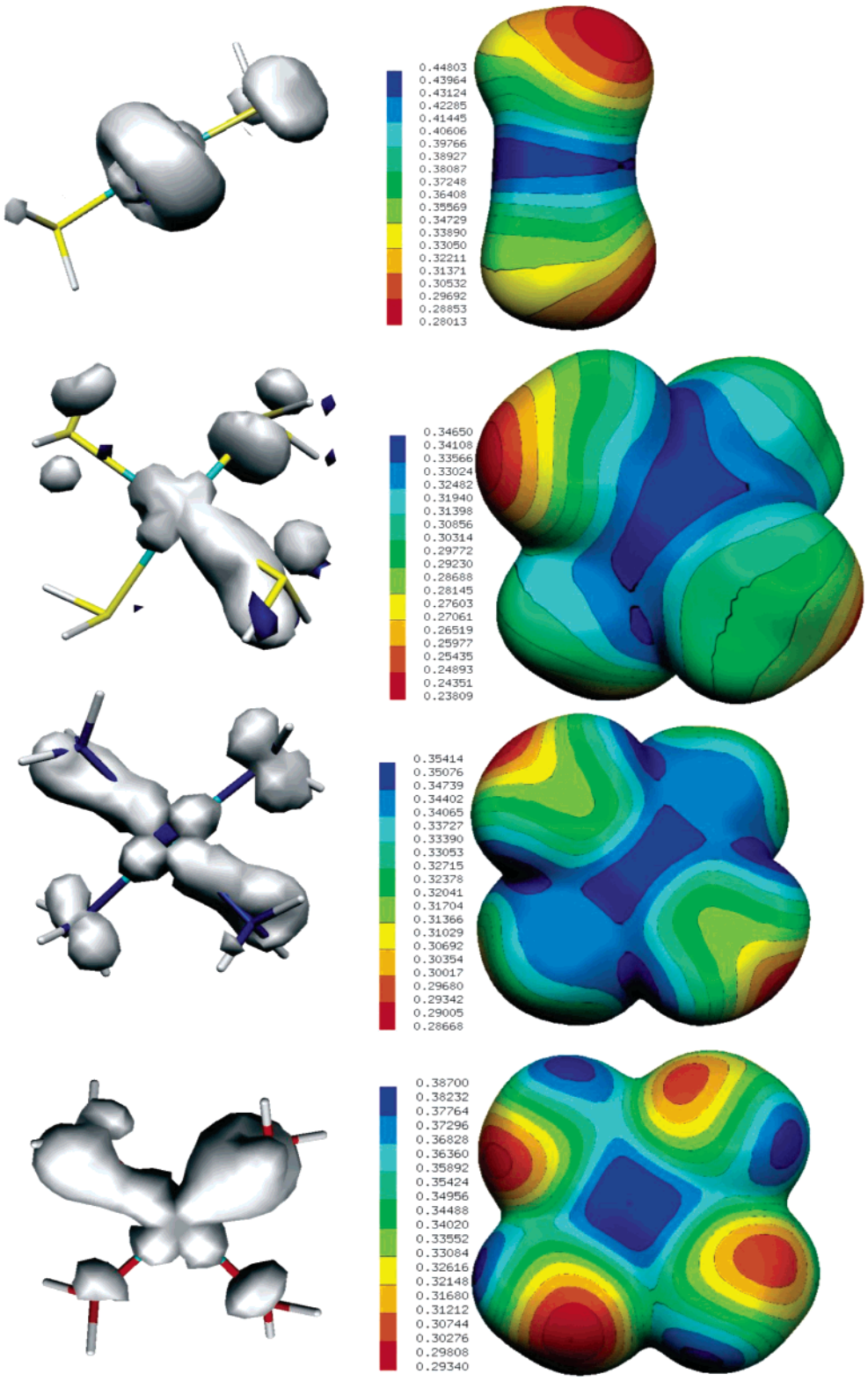

Figure 12. Plots of spin densities and maps of electrostatic potentials for the disulfide, square-planar tetraaqua, tetraamine, and tetrasulfide Cu(II) complexes. The extrema of the maps (in electronvolts) are as follows: $[Cu(H_2S)_2]^{2+}$ $V_{min} = 0.28$, $V_{max} = 0.45$; $[Cu(NH_3)_4]^{2+}$ $V_{min} = 0.27$, $V_{max} = 0.35$; $[Cu(H_2O)_4]^{2+}$ $V_{min} = 0.29$, $V_{max} = 0.39$; $[Cu(H_2S)_4]^{2+}$ $V_{min} = 0.24$, $V_{max} = 0.35$.

in the studied systems. Furthermore, the different energy evaluations may be useful when the presented results are to be compared with other methods, namely, the force fields.

The Cu(I) systems prefer a coordination number of 2 (followed by 3 and 4) in the presence of the ammine and aqua ligand field. The 3- and 4-coordinated structures are favored when the H_2S molecules occupy the first solvation shell. For the divalent copper compounds, the 4- and 5-coordinated structures represent the most stable forms.

The highest stabilization energies were found for ammine ligands followed by hydrogen sulfide and aqua ligands in the case of the Cu(I) complexes. The order of the last two ligands is inverted in the Cu(II) systems due to a higher electrostatic contribution to the stabilization energy.

On the basis of the MO and NBO analysis, the largest dative contribution to the Cu−X bond occurs in the sulfur case followed by nitrogen. The weakest donor ability is exhibited by oxygen. It is in agreement with the order of the softness parameter from the HSAB principle. This can explain the higher coordination of the Cu^+ cations in sulfide-containing complexes. Another reason the water molecules often escape to the second solvation shell is linked to a non-negligible energy release by the formation of strong H-bonds with other polarized ligands (either NH_3 or H_2O). Therefore, the final arrangement of the ligand molecules in solvation shells is a consequence of several factors. In the case of more polar molecules (NH_3 and H_2O in the present study), the system can be stabilized by the formation of both dative bonds and H-bonds. Lower coordination prevails when the H-bonding is accompanied by a sufficient energy release. The dative bonding is preferable in the presence of less polar H_2S molecules where only very weak H-bonds can be formed.

The revealed preference can be generalized as follows: nitrogen-containing ligands (like histidine) form stronger bonds with the copper cations than the Cu−S bonds in, for example, cysteine or methionine and the Cu−O coordination with, for example, serine or tyrosine. However, this preference must be taken with care, since the remaining part of the ligated molecule can mask electron-density characteristics substantially.

Both vertical IP_{vert} and adiabatic IP_{adiab} ionization potentials (as well as electron affinities, EA) were calculated to describe possible transitions between the Cu(I) and Cu(II) oxidation states. The highest IP values were obtained for the complexes containing the H_2S molecules.

The partial charges were computed by the NPA method. The partial charge located on the Cu atom corresponds to the extent of the total donation. The copper 4s AO is the main target of the donation effects. Therefore, its occupation was observed. In the Cu(II) complexes, the occupation numbers of the Cu 3d AOs also need to be considered.

The presented data provide a systematic and wide set of structures and energies of Cu-containing clusters of biological relevance. The data can be used to rationalize selected aspects of the physical chemistry of Cu interactions in biopolymers and can also be used for calibration of other computational methods such as Cu-containing force fields. To simplify this task, all studied structures are available as Supporting Information.

Acknowledgment. This study was supported by Charles University grant 438/2004/B_CH/MFF, grant NSF-MŠMT ČR 1P05 ME-784, and grant MSM 0021620835. J.Š. acknowledges support by grant 203/05/0388, Grant Agency of the Czech Republic. The Institute of Biophysics is supported by grant AVOZ50040507, Ministry of Education of the Czech Republic. The computational resources from Meta-Centers in Prague, Brno, and Pilsen are acknowledged for access to their excellent supercomputer facilities.

Supporting Information Available: Tables showing the coordinates of the examined structures and figures showing MOs. This material is available free of charge via the Internet at http://pubs.acs.org.

References and Notes

(1) Siegbahn, P. E. M.; Wirstam, M. *J. Am. Chem. Soc.* **2001**, *123*, 11819.
(2) Prabhakar, R.; Siegbahn, P. E. M. *J. Phys. Chem. B* **2003**, *107*, 3944.
(3) Wang, X.; Berry, S. M.; Xia, Y.; Lu, Y. *J. Am. Chem. Soc.* **1999**, *121*, 7449.
(4) Palmer, A. E.; Randall, D. W.; Xu, F.; Solomon, E. I. *J Am. Chem. Soc.* **1999**, *121*, 7138.
(5) Randall, D. W.; George, S. D.; Hedman, B.; Hodgson, K. O.; Fujisawa, K.; Solomon, E. I. *J. Am. Chem. Soc.* **2000**, *122*, 11620.
(6) Randall, D. W.; George, S. D.; Holland, P. L.; Hedman, B.; Hodgson, K. O.; Tolman, W. B.; Solomon, E. I. *J. Am. Chem. Soc.* **2000**, *122*, 11632.
(7) Holland, P. L.; Tolman, W. B. *J. Am. Chem. Soc.* **2000**, *122*, 6331.
(8) Holland, P. L.; Tolman, W. B. *J. Am. Chem. Soc.* **1999**, *121*, 7270.
(9) Gray, H. B.; Malmstroem, B. G.; Williams, R. J. P. *J. Biol. Inorg. Chem.* **2000**, *5*, 551.
(10) Olsson, M. H. M.; Hong, G. Y.; Warshel, A. *J. Am. Chem. Soc.* **2003**, *125*, 5025.
(11) Olsson, M. H. M.; Ryde, U. *J. Biol. Inorg. Chem.* **1999**, *4*, 654.
(12) Olsson, M. H. M.; Ryde, U.; Roos, B. O.; Pierloot, K. *J. Biol. Inorg. Chem.* **1998**, *3*, 109.
(13) Ryde, U.; Olsson, M. H. M.; Roos, B. O.; De Kerpel, J. O. A.; Pierloot, K. *J. Biol. Inorg. Chem.* **2000**, *5*, 565.
(14) Book, L. D.; Arnett, D. C.; Hu, H.; Scherer, N. F. *J. Phys. Chem. A* **1998**, *102*, 4350.
(15) Fraga, E.; Webb, M. A.; Loppnow, G. R. *J. Phys. Chem.* **1996**, *100*, 3278.
(16) Sabolovic, J.; Liedl, K. R. *J. Am. Chem. Soc.* **1999**.
(17) Sabolovic, J.; Tautermann, C. S.; Loerting, T.; Liedl, K. R. *Inorg. Chem.* **2003**, *42*, 2268.
(18) Katz, A.; Shimoni-Livny, L.; Navon, O.; Navon, N.; Bock, C.; Glusker, J. *Helv. Chim. Acta* **2003**, *86*, 1320.
(19) Rulíšek, L.; Havlas, Z. *J. Am. Chem. Soc.* **2000**, *122*, 10428.
(20) Rulíšek, L.; Havlas, Z. *J. Phys. Chem. A* **2002**, *106*, 3855.
(21) Rulíšek, L. *Chem. Listy* **2002**, *96*, 132.
(22) Rulíšek, L.; Havlas, Z. *J. Phys. Chem. B* **2003**, *107*, 2376.
(23) Bertran, J.; Rodrigues-Santiago, L.; Sodupe, M. *J. Phys. Chem. B* **1999**, *103*, 2310.
(24) Shoeib, T.; Rodriquez, C. F.; Siu, K. W. M.; Hopkinson, A. C. *Phys. Chem. Chem. Phys.* **2001**, *3*, 853.
(25) Caraiman, D.; Shoeib, T.; Siu, K.; Hopkinson, A.; Bohme, D. *Int. J. Mass Spectrom.* **2003**, *228*, 629.
(26) Santra, S.; Zhang, P.; Tan, W. *J. Phys. Chem. A* **2000**, *104*, 12021.
(27) Manikandan, P.; Epel, B.; Goldfarb, D. *Inorg. Chem.* **2001**, *40*, 781.
(28) Shimizu, K.; Maeshima, H.; Yoshida, H.; Satsuma, A.; Hattori, T. *Phys. Chem. Chem. Phys.* **2001**, *3*, 862.
(29) Sigman, J. A.; Kwok, B. C.; Gengenbach, A.; Lu, Y. *J Am. Chem. Soc.* **1999**, *121*, 8949.
(30) Hackl, E. V.; Kornilova, S. V.; Kapinos, L. E.; Andruschenko, V. V.; Galkin, V. L.; Grigoriev, D. N.; Blagoi, Y. P. *J. Mol. Struct.* **1997**, *408*, 229.
(31) Hemmert, C.; Pitie, M.; Renz, M.; Gornitzka, H.; Soulet, S.; Meunier, B. *J. Biol. Inorg. Chem.* **2001**, *6*, 14.
(32) Herrero, L. A.; Terron, A. *J. Biol. Inorg. Chem.* **2000**, *5*, 269.
(33) Meggers, E.; Holland, P. L.; Tolman, W. B.; Romesberg, F. E.; Schultz, P. G. *J. Am. Chem. Soc.* **2000**, *122*, 10714.
(34) Atwell, S.; Meggers, E.; Spraggon, G.; Schultz, P. G. *J. Am. Chem. Soc.* **2001**, *123*, 12364.
(35) Schoentjes, B.; Lehn, J.-M. *Helv. Chim. Acta* **1995**, *78*, 1.
(36) Lamsabhi, A.; Alcami, M.; Mo, O.; Yanez, M.; Tortajada, J. *ChemPhysChem* **2004**, *5*, 1871.
(37) Gasowska, A.; Lomozik, L. *Monatsh. Chem.* **1995**, *126*, 13.
(38) Burda, J. V.; Šponer, J.; Hobza, P. *J. Phys. Chem.* **1996**, *100*, 7250.
(39) Burda, J. V.; Šponer, J.; Leszczynski, J.; Hobza, P. *J. Phys. Chem. B* **1997**, *101*, 9670.
(40) Šponer, J.; Sabat, M.; Burda, J.; Leszczynski, J.; Hobza, P.; Lippert, B. *J. Biol. Inorg. Chem.* **1999**, *4*, 537.
(41) Noguera, M.; Bertran, J.; Sodupe, M. *J. Phys. Chem. A* **2004**, *108*, 333.
(42) Rulíšek, L.; Šponer, J. *J. Phys. Chem. B* **2003**, *106*, 1913.
(43) Burda, J. V.; Shukla, M. K.; Leszczynski, J. *J. Mol. Model.* **2005**, *11*, 362.
(44) Tachikawa, H. *Chem. Phys. Lett.* **1996**, *260*, 582.
(45) Hamilton, I. P. *Chem. Phys. Lett.* **2004**, *390*, 517.
(46) Feller, D.; Glendening, E. D.; de Jong, W. A. *J. Chem. Phys.* **1999**, *110*, 1475.
(47) Schroeder, D.; Schwartz, H.; Wu, J.; Wesdemiotis, C. *Chem. Phys. Lett.* **2001**, *343*, 258.
(48) Marini, G. W.; Liedl, K. R.; Rode, B. M. *J. Phys. Chem. A* **1999**, *103*, 11387.
(49) Schwenk, C.; Rode, B. *ChemPhysChem* **2004**, *5*, 342.
(50) Schwenk, C. F.; Rode, B. M. *Phys. Chem. Chem. Phys.* **2003**, *5*, 3418.
(51) Pranowo, H. *Chem. Phys.* **2003**, *291*, 153.

(52) Berces, A.; Nukada, T.; Margl, P.; Ziegler, T. *J. Phys. Chem. A* **1999**, *103*, 9693.
(53) Pranowo, H. D.; Rode, B. M. *J. Phys. Chem. A* **1999**, *103*, 4298.
(54) Pranowo, H. D.; Setiajin, A. H. B.; Rode, B. M. *J. Phys. Chem. A* **1999**, *103*, 11115.
(55) Pranowo, H. D.; Rode, B. M. *Chem. Phys.* **2001**, *263*, 1.
(56) Haeffner, F.; Brinck, T.; Haeberlein, M.; Moberg, C. *Chem. Phys. Lett.* **1997**, *397*, 39.
(57) Cordeiro, N. M. D. S.; Gomes, J. A. N. F. *J. Comput. Chem.* **1993**, *14*, 629.
(58) Subramanian, V.; Shankaranarayanan, C.; Nair, B. U.; Kanthimathi, M.; Manickkavachagam, R.; Ramasami, T. *Chem. Phys. Lett.* **1997**, *274*, 275.
(59) Gresh, N.; Policar, C.; Giessner-Prettre, C. *J. Phys. Chem.* **2002**, *106*, 5660.
(60) Ledecq, M.; Lebon, F.; Durant, F.; Giessner-Prettre, C.; Marquez, A.; Gresh, N. *J. Phys. Chem. B* **2003**, *107*, 10640.
(61) Schwerdtfeger, P.; Krawczyk, R. P.; Hammerl, A.; Brown, R. *Inorg. Chem.* **2004**, *43*, 6707.
(62) Neese, F. *Magn. Reson. Chem.* **2004**, *42*, S187.
(63) Konopka, M.; Rousseau, R.; Stich, I.; Marx, D. *J. Am. Chem. Soc.* **2004**, *126*, 12103.
(64) Bauschlicher, C. W.; Langhoff, S. R.; Partridge, H. *J. Chem. Phys.* **1991**, *94*, 2068.
(65) Burda, J. V.; Pavelka, M.; Simanek, M. *J. Mol. Struct.* **2004**, *683*, 183.
(66) Pavelka, M.; Burda, J. V. *Chem. Phys.* **2005**, *312*, 193.
(67) Hurley, M. M.; Pacios, L. F.; Christiansen, P. A.; Ross, R. B.; Ermler, W. C. *J. Chem. Phys.* **1986**, *84*, 6840.
(68) The usage of the originally suggested pseudoorbitals leads to a wrong description of the basic physical properties, such as the IP or EA, of the copper atom. Here, at least qualitative agreement can be obtained when original orbitals are augmented with diffuse and polarization functions.
(69) Poater, J.; Sola, M.; Rimola, A.; Rodriguez-Santiago, L.; Sodupe, M. *J. Phys. Chem. A* **2004**, *108*, 6072.
(70) Boys, S. F.; Bernardi, F. *Mol. Phys.* **1970**, *19*, 553.
(71) Tiraboschi, G.; Roques, B.-P.; Gresh, N. *J. Comput. Chem.* **1999**, *20*, 1379.
(72) Tiraboschi, G.; Gresh, N.; Giessner-Prettre, C.; Pedersen, L. G.; Deerfield, D. W. *J. Comput. Chem.* **2000**, *21*, 1011.
(73) Šponer, J.; Burda, J. V.; Sabat, M.; Leszczynski, J.; Hobza, P. *J. Phys. Chem. A* **1998**, *102*, 5951.
(74) Ostlund, N. S.; Sabo, A. *Modern Quantum Chemistry*; McGraw-Hill: New York, 1989.
(75) Zakrzewski, V. G.; Ortiz, J. V. *Int. J. Quantum Chem.* **1995**, *53*, 583.
(76) Reed, A. E.; Weinstock, R. B.; Weinhold, F. *J. Chem. Phys.* **1985**, *83*, 735.
(77) Frisch, M. J.; Trucks, G. W.; Schlegel, H. B.; Scuseria, G. E.; Robb, M. A.; Cheeseman, J. R.; Zakrzewski, V. G.; Montgomery, J. A., Jr.; Stratmann, R. E.; Burant, J. C.; Dapprich, S.; Millam, J. M.; Daniels, A. D.; Kudin, K. N.; Strain, M. C.; Farkas, O.; Tomasi, J.; Barone, V.; Cossi, M.; Cammi, R.; Mennucci, B.; Pomelli, C.; Adamo, C.; Clifford, S.; Ochterski, J.; Petersson, G. A.; Ayala, P. Y.; Cui, Q.; Morokuma, K.; Malick, D. K.; Rabuck, A. D.; Raghavachari, K.; Foresman, J. B.; Cioslowski, J.; Ortiz, J. V.; Stefanov, B. B.; Liu, G.; Liashenko, A.; Piskorz, P.; Komaromi, I.; Gomperts, R.; Martin, R. L.; Fox, D. J.; Keith, T.; Al-Laham, M. A.; Peng, C. Y.; Nanayakkara, A.; Gonzalez, C.; Challacombe, M.; Gill, P. M. W.; Johnson, B. G.; Chen, W.; Wong, M. W.; Andres, J. L.; Head-Gordon, M.; Replogle, E. S.; Pople, J. A. *Gaussian 98*, revision A.1x; Gaussian, Inc.: Pittsburgh, PA, 2001.
(78) Weinhold, F. *NBO 5.0*; University of Wisconsin: Madison, WI, 2001.
(79) Schaftenaar, G. *Molden*, version 3.9 (http://www.cmbi.kun.nl/~schaft/molden/molden.html).
(80) Flükiger, P. F. http://www.cscs.ch/molekel/.
(81) Portmann, S.; Lüthi, H. P. *Chimia* **2000**, *54*, 766.
(82) Parr, R. G.; Pearson, R. G. *J. Am. Chem. Soc.* **1983**, *105*, 7512.
(83) Kothekar, V.; Pullman, A.; Demoulin, D. *Int. J. Quantum Chem.* **1979**, *14*, 779.
(84) Gresh, N. *J. Comput. Chem.* **1995**, *16*, 856.
(85) Gresh, N.; Stevens, W. J.; Krauss, M. *J. Comput. Chem.* **1995**, *16*, 843.
(86) Piquemal, J. P.; Gresh, N.; Giessner-Prettre, C. *J. Phys. Chem. A* **2003**, *107*, 10353.
(87) Taylor, M.; Muntean, F.; Lineberger, W.; McCoy, A. *J. Chem. Phys.* **2004**, *121*, 5688.
(88) Lee, S. U.; Han, Y. K. *J. Mol. Struct.* **2004**, *672*, 231.
(89) Satta, M.; Di Palma, T. M.; Paladini, A.; Giardini Guidoni, A. *Appl. Surf. Sci.* **2002**, *168*, 215.
(90) Webelements. http://www.webelements.com/webelements/elements/text/Cu/thdyn.html.
(91) Parr, R. G.; Yang, W. *Density Functional Theory of Atoms and Molecules*; Oxford University Press: Oxford, U.K., 1989.
(92) Zimmermann, T.; Zeizinger, M.; Burda, J. V. *J. Inorg. Biochem.* **2005**, *99*, 2184.